

LUT UNIVERSITY
LUT School of Energy Systems
LUT Mechanical Engineering

Juuso Lindroos

**LONGITUDINAL STRENGTH DESIGN OF AN ICE STRENGTHENED
CONTAINER SHIP USING HIGH STRENGTH STEEL AND ITS EFFECTS ON
FATIGUE STRENGTH**

15.5.2020

Examiners: Professor Timo Björk
M. Sc. (Tech.) Ville Valtonen

TIIVISTELMÄ

LUT-Yliopisto
LUT School of Energy Systems
LUT Kone

Juuso Lindroos

Longitudinal strength design of an ice strengthened container ship using high strength steel and its effects on fatigue strength

Diplomityö

2020

87 sivua, 18 kuvaa, 14 taulukkoa ja 5 liitettä

Tarkastajat: Professori Timo Björk
DI Ville Valtonen

Hakusanat: Suurlujuusteräs, konttialuksen suunnittelu, 4R-menetelmä, rungon painosäästö

Tämän tutkimuksen tavoitteena on suunnitella jäävahvistetun konttialuksen pitkäikäisyys käyttäen suunnittelussa myötölujuudeltaan 690 MPa olevaa terästä. Motivaatio työn tekemiseen on mahdollisuus keventää aluksen painoa käyttämällä vähemmän terästä aluksen valmistuksessa verrattuna nykyisiin aluksiin. Tämän lisäksi työssä tutkitaan suurlujuusteräksen käytön vaikutusta aluksen väsymiskestoikään. Lopuksi työssä verrataan kahden keskilaivapoikkileikkauksen painoja, joista toinen on suunniteltu käyttäen myötölujuudeltaan 460 MPa lujuusluokan ja toinen käyttäen 690 MPa lujuusluokan terästä.

Suunnittelu perustuu UR-S11A dokumentin mukaisiin raja-arvoihin. Suunnittelua varten 690 MPa teräkselle on käytetty uutta materiaalikertoimen arvoa, sillä nykyiset suunnittelumetodit eivät tunnista kyseistä suurlujuusterästä. Teräksen käytön vaikutusta väsymiskestoikään tarkastellaan käyttämällä 4R väsymislaskentamenetelmää. Menetelmä huomioi teräksen lujuuden ja jäännösjännitysten vaikutuksen väsymiskestoikää laskettaessa.

Työssä päädyttiin lopputulokseen, että konttialus voidaan suunnitella käyttäen UR-S11A mukaisia raja-arvoja. Näistä raja-arvoista keksiläivan poikkileikkauksen jäyhyys on suunnittelua eniten rajaava tekijä. Teräksen lujuusluokan kasvattamisen todettiin laskevan laivan väsymiskestoikää huomattavasti. Hitsin jälkikäsitteilyn avulla väsymiskestoikä voitiin kuitenkin nostaa jopa korkeammaksi verrattuna 470 MPa lujuusluokasta teräksestä suunnitellun poikkileikkauksen väsymiskestoikään. Lopputuloksena myötölujuudeltaan 690 MPa terästä käyttämällä päästiin noin 14% painosäästöön verrattuna myötölujuudeltaan 460 MPa teräksen käyttöön konttialuksen poikkileikkauksessa. Lähes kaikki painosäästö saatiin aikaiseksi käyttämällä jäävahvistuksissa 690 MPa myötölujuuden terästä 460 MPa myötölujuuden teräksen sijaan.

ABSTRACT

LUT University
LUT School of Energy Systems
LUT Mechanical Engineering

Juuso Lindroos

Longitudinal strength design of an ice strengthened container ship using high strength steel and its effects on fatigue strength

Master's thesis

2020

87 pages, 18 figures, 14 tables and 5 appendices

Examiners: Professor Timo Björk
M. Sc. (Tech.) Ville Valtonen

Keywords: High strength steel, container ship design, 4R-method, hull weight savings

The aim of this thesis is to design the longitudinal strength of an ice strengthened container ship when using steel with yield strength of 690 MPa. Motivation for using high strength steel is the possibility to use less steel in hull construction. The use of less steel could bring weight savings compared to current designs. The thesis also studies on possible reduction of fatigue life when introducing steel with yield strength of 690 MPa into the design. Finally, possible weight savings are calculated by comparing the unit weight of two similar midship section, one made using steel with yield strength of 460 MPa and one using steel with yield strength of 690 MPa.

Designing process of the midship section using 690 MPa steel is based on UR-S11A document. A new material factor value for the steel with yield strength of 690 MPa is used in the design process as the current rules do not provide guidance on using 690 MPa steel. In order to study the change on fatigue life when using steel with 690 MPa, a 4R fatigue calculation method is used. With the method the effects of material strength and residual stresses on fatigue life can be considered.

It is found out that a container ship can be designed using steel with yield strength of 690 MPa by following UR-S11A limits for permissible stress and moment of inertia. It was found out that the moment of inertia limit drives the design process. A significant reduction on fatigue life was calculated when using steel with yield strength of 690 MPa compared to the use of 460 MPa steel. By applying HFMI post weld treatment, the fatigue life of midship section with 690 MPa steel could be increased to be even higher than the fatigue life of midship section made using 460 MPa steel. Finally, it was calculated that around 14% weight loss could be achieved by using 690 MPa steel. Most of the weight saving were obtained by reducing the scantlings of ice strengthening structure.

ACKNOWLEDGEMENTS

I want to thank my examiner at LUT Professor Timo Björk for providing guidance in the thesis process and providing valuable help in difficult details. Thank you for providing important knowledge in the thesis project and through out the university studies in the field of steel structures.

I would especially like to address my acknowledgements to my supervisor M. Sc. Ville Valtonen from Aker Arctic Technology for guiding me in aspects that were relatively new to me in the beginning and providing me help in every problem I had. There was always time for questions and conversations even in the busiest times. In addition, I want to thank Rob Hindley from Aker Arctic Technology for giving good points of views to the thesis and providing valuable connections to the industry.

Last, but definitely not least, I want to thank Rob Tustin from Lloyd's Register. Thank you for providing me knowledge from the class point of view and sharing expertise in ship design. Additionally, I want to thank Soon Jo Hong from Lloyd's Register for sharing expertise and guiding in container ship design. Also, I want to thank Dong-Yeon Lee for providing assistance in ship fatigue aspects.

Juuso Lindroos

In Lappeenranta 15.5.2020

TABLE OF CONTENTS

TIIVISTELMÄ	1
ABSTRACT.....	2
ACKNOWLEDGEMENTS	3
TABLE OF CONTENTS	5
LIST OF SYMBOLS AND ABBREVIATIONS	7
1 INTRODUCTION	11
1.1 Background.....	12
1.2 Motivation for the research.....	12
1.3 Research objectives.....	15
1.4 Research problem and research questions	15
1.5 Scope of research	16
1.5.1 Exclusions in the research.....	17
1.6 Hypothesis	19
2 PRINCIPLES OF GLOBAL LOADS AND CRITICAL LOCATIONS IN CONTAINER SHIP CONSTRUCTION	21
2.1 Design principles of ship structural design.....	21
2.1.1 Reliability-based design.....	21
2.1.2 Rationally-based design.....	24
2.2 Longitudinal loads acting on the ship’s hull.....	24
2.2.1 Still water bending moment.....	26
2.2.2 Wave bending moments.....	29
2.3 Steel grade in strength design	31
2.4 Critical fatigue locations in container ship midship section.....	33
2.5 Possible fatigue issues when moving to high strength steels.....	35
3 METHODOLOGY	37
3.1 Rule sets and design guides used in the study	39
3.2 Main dimensions and initial midship section using AH47 steel.....	39
3.3 Longitudinal strength assessment	41
3.3.1 Still water bending moment.....	43
3.3.2 Vertical wave bending moment	44

3.3.3	Hull girder stress	45
3.4	Scantling design using RulesCalc	46
3.5	High strength steel scantling design	48
3.6	Locations for fatigue assessment	49
3.7	Rule based fatigue life	52
3.8	4R method.....	55
3.8.1	Stress concentration factors for 4R calculations.....	60
3.9	Unit weight calculation	63
4	RESULTS	64
4.1	Global loads acting on the ship with AH47 midship section.....	64
4.1.1	Still water and wave bending moments	64
4.2	Midship section designed using AH70 steel.....	65
4.2.1	Hull girder stress according UR-S11A	66
4.3	Rule based fatigue life calculations	67
4.4	Stress concentration factors	67
4.5	4R fatigue life calculations	69
4.6	Comparison of fatigue lives	71
4.7	Unit weights.....	72
5	ANALYSIS AND DISCUSSION	73
5.1	Analysis of key results	73
5.2	Discussion of results	75
5.2.1	Further study to be conducted.....	79
6	CONCLUSIONS	81
	LIST OF REFERENCES	83
APPENDIX		
Appendix I:	UR-S11A section modulus and stress calculations.	
Appendix II:	Drawings of midship section made using AH47 steel.	
Appendix III:	Drawings of midship section made using AH70 high strength steel.	
Appendix IV:	Transverse bulkhead drawing.	
Appendix V:	Stress concentration FEA results.	

LIST OF SYMBOLS AND ABBREVIATIONS

A	Immersed area [m ²]
A_{DK}	Projected area of the uppermost deck [m ²]
A_{WL}	Area at waterline [m ²]
B	Molded breadth of ship [m]
b	Buoyancy pressure [Pa]
C_b	Block coefficient
C_w	Wave coefficient
C_{4R}	Characteristic fatigue capacity
D_e	Elementary fatigue damage
E	Young's modulus [N/mm ²]
f_{bow}	Bow flare shape coefficient
f_c	Correction factor
f_m	Distribution factor along the length for still water bending moment
f_{mean}	Means stress coefficient
f_{NL}	Wave bending moment non-linear correction factor
f_p	Adjustment factor for wave-induced loads
f_{p-sw}	Coefficient for still water bending moment
f_R	Fraction of ships lifetime spent in transit
f_{SW}	Distribution factor for still water bending moment
f_t	Ratio between scantling draught and draught at loading condition
f_{thick}	Thickness coefficient
f_{warp}	Warping coefficient
H	Strength coefficient [N/mm ²]
I_{net}	Net moment of inertia [m ⁴]
K_a	Stress concentration factor
k_L	Material factor
$K_{s.b}$	Structural stress concentration factor for bending loading
$K_{s.m}$	Structural stress concentration factor for membrane loading
$K_{t.b}$	Effective notch stress concentration factor for bending loading
$K_{t.m}$	Effective notch stress concentration factor for membrane loading

$K1$	S-N curve coefficient
$K2$	S-N curve coefficient
L	Rule length of ship [m]
L_{pp}	Length between perpendiculars [m]
M	Bending moment [kNm]
M_s	Still water bending moment [kNm]
$M_{sw-h-min}$	Minimum still water bending moment [kNm]
M_w	Rule wave bending moment [kNm]
M_{wv-f}	Rule wave bending moment in fatigue calculations [kNm]
$M_{wv-h-min}$	Vertical wave bending moment [kNm]
m_{4R}	S-N curve slope
N_f	Cycles to failure [n]
N_D	Number of wave cycles during the design fatigue lifetime [n]
N_r	Corresponding number of cycles to probability of exceedance [n]
n	Strain hardening exponent
R	Applied stress ratio
R_d	Design resistance [MPa]
R_{eh}	Yield strength of material [N/mm ²]
R_k	Characteristic resistance effect [MPa]
R_{local}	Local stress ratio
S	Nominal stress [N/mm ²]
S_d	Design load effect [MPa]
S_k	Characteristic load effect [MPa]
t	Plate thickness [mm]
T	Design draught [m]
T_D	Design life of the ship [a]
T_F	Fatigue life [a]
V	Shear force [N]
v	Coefficient for elementary fatigue damage
W	Unit weight of midship section [kg/m]
w	Weight pressure [Pa]
$W\%$	Weight loss
Z	Vertical distance from the baseline of the location under consideration [m]

z_f	Vertical distance between the uppermost deck and the waterline at forward perpendicular [m]
Z_n	Vertical distance from the baseline to the neutral axis [m]
α	Fraction in each loading condition
$\Gamma(x)$	Complete gamma function
γ_f	Load safety factor
γ_m	Material safety factor
γ_s	Partial safety factor
γ_w	Partial safety factor
$\gamma(x,y)$	Incomplete Gamma function
γ_1	Partial safety factor for material
γ_2	Partial safety factor for load combinations
Δm	Change in inverse S-N curve slope at 10^7 cycles
$\Delta \varepsilon$	Strain range
$\Delta \sigma_b$	Bending stress range [N/mm ²]
$\Delta \sigma_{FS}$	Fatigue stress range [N/mm ²]
$\Delta \sigma_{HS}$	hull girder stress range [N/mm ²]
$\Delta \sigma_k$	Effective notch stress method stress range [N/mm ²]
$\Delta \sigma_{limit}$	Limit stress range for fatigue [N/mm ²]
$\Delta \sigma_m$	Membrane stress range [N/mm ²]
$\Delta \sigma_q$	Stress range at intersection of S-N curve segments [N/mm ²]
ζ	Weibull shape parameter
μ	Coefficient for change of inverse slope of S-N curve
σ_b	Secondary bending stress [N/mm ²]
σ_{HOG}	Combined design stress [N/mm ²]
σ_{HS}	Hull girder hot spot stress [N/mm ²]
σ_L	Normal stress [N/mm ²]
σ_k	Effective notch stress [N/mm ²]
σ_m	Nominal stress [N/mm ²]
σ_{mean}	Mean stress [N/mm ²]
σ_p	Notch stress [N/mm ²]
σ_{perm}	Permissible stress [N/mm ²]
σ_{res}	Residual stress [N/mm ²]

σ_s	Structural stress [N/mm ²]
AH47	Steel with yield strength of 460 MPa
AH70	High strength steel with yield strength of 690 MPa
ALS	Accidental limit state
CSR	Common Structural Rules
EEDI	Energy Efficiency Design Index
ENS	Effective Notch Stress method
FDA	Fatigue Design Assessment
FEA	Finite Element Analysis
FLS	Fatigue limit state
HFMI	High Frequency Mechanical Impact
HHI	Hyundai Heavy Industries
IACS	International Association of Classification Societies
IMO	International Maritime Organization
LR	Lloyd's Register
LRFD	Load and Resistance Factored Design
PSF	Partial Safety Factor method
SDDG	Structural Detail Design Guide
SLS	Serviceability limit state
TEU	Twenty-foot equivalent unit
ULS	Ultimate limit state
ULCS	Ultra Large Container Ship
WSM	Working Stress Method

1 INTRODUCTION

Ships are usually constructed out of steel and ship's steel hull creates a major part of the ships weight. By reducing the steel weight, costs and environmental impact of shipping could be lowered. There are number of ways to reduce ship's weight, one is to use steels with higher strength in thin plates of hull construction rather than using thicker plates with lower strength steel. Lower strength steel in thick plates is sometimes used due to rule limitations for using high strength steel and lower price compared to higher strength steels.

This thesis work focuses on finding ways how to design an ice strengthened container ship when using high strength steel as a construction material for ship's hull. High strength steel considered in the study has a yield strength of 690 MPa. Currently highest yield strength recognized by International Association of Classification Societies (IACS) is a yield strength of 390 MPa (UR-S4 2010, p. 1). The same highest yield strength is noted by Lloyd's Register (LR) to be highest yield strength allowed for steel to be used in any hull construction. LR also allows the use of steel with yield strength of 460 MPa in special locations in a container ship hull construction. (Lloyd's Register 2019, p. 176.)

Design of a ship using high strength steel cannot lay on the given rules as there are no design guide for using such high strength steel. The procedure of designing a container ship using high strength steel with yield strength of 690 MPa in hull construction is studied and different locations are considered where it would be beneficial to use steels with such high yield strength. These parts of the midship section can be areas with high stresses or stress concentrations.

Use of high strength steel in the hull can lead to fatigue problems as the materials fatigue capacity is not expected to increase even if the static capacity increases. Ships are naturally prone to fatigue as they operate in an environment that creates cyclic loading. Fatigue life of the design ship is determined by using a fatigue model developed at LUT University called 4R method. This method includes the local stress range in a critical location as well as residual stresses in the material, weld radius in a joint and material strength. The 4R method is described more in more detail in Chapter 3.8.

1.1 Background

A Finnish ship design company Aker Arctic Technology is taking part to a project to research the possibility to use high-tensile steels as a construction material for ship's hull. Steel manufacturers are becoming more capable of producing large quantities of high-tensile steels for a reasonable price to be used in ship construction. The use of high-tensile steel can significantly lower the amount of steel needed to construct a ship. This creates a possibility to lower the environmental impact of shipping by using less fuel and by lowering the amount of steel needed to be made for the construction of the ship. The cost of operation could be also lowered due lower fuel consumption as lower steel use.

Ships operate in an environment which produces a lot of cyclic loading to the ship's hull. This cyclic loading is produced by waves, that the ship encounters almost during its entire lifetime. In addition to these wave-induced loads, ships are subjected to still water loads. The still water loads depend on the loading and hull form of the ship and they change as the loading of the ship's changes. The still water loads can also be cyclic like in a tanker ship, that sails one transit in a full cargo and returns without cargo in ballast condition.

These cyclic loads acting against the ship's hull subject the structural members to fatigue. This fatigue can lead to a failure of the structural members. For this reason, the structural design is currently checked against fatigue in order to make sure that the design does not fail due to fatigue during the ships intended operational lifetime. The fatigue check is usually performed according to the rules of a classification society in order to ensure the ships safety during the entire lifetime.

Currently ships are mainly constructed of steels with highest yield strength of 355 MPa. In some parts of the ship 460 MPa steel may be used to improve the strength of a structural member in locations where high stresses are present. This is partly due to steel manufacturers lack of capability to produce high quantities of high-tensile steels at a reasonable price that could be used in ship construction.

1.2 Motivation for the research

Motivation for the research is to create method to lower ship's weight by using higher strength steel. The weight reduction can lead to lower fuel usage and lower the

environmental impact of shipping. Ships are an important mean of transport when transporting freight around the globe, as United Nations (2019, p. 4) reviewed that measured by the volume of transported freight, four fifths of all transport happens by sea. Ships can transport large amounts of cargo for long distances in global trade regardless of them being quite slow compared to other means of transporting goods i.e. air freight.

The use of 690 MPa steel could bring additional benefits to the main motivation of the study. These benefits also motivate the study. The benefits that can be assumed are listed in Table 1. The use of 690 MPa steel is also assumed to have challenges together with the benefits. The assumed challenges are also listed in Table 1. The items that are considered to have the most benefits are described in more detail after the table.

Table 1. Assumed benefits and challenges of using 690 MPa steel

Benefits:	Challenges:
Reduction of ship's weight	Rule limitations on high strength steels
Reduction in fuel consumption	Rule limitations of cross section properties and scantlings
Reduced costs of operation	Design process when using 690 MPa steel
Reduced cost of manufacturing	Availability of 690 MPa steel
Reduced environmental impact of operation	Price of 690 MPa steel
Improved Energy Efficiency Design Index (EEDI) value	Construction from steel with yield strength of 690 MPa
Reduced environmental impact of construction	Shipwrecking and recycling of the material
Improved working conditions at shipyard	

The global warming is making it possible to use polar and arctic regions for transport, so it is important that the environmental impact of shipping is as low as possible when entering these new environments. As the International Maritime Organization (IMO) states in the INTERNATIONAL CODE FOR SHIPS OPERATING IN POLAR WATERS, POLAR CODE (2014, p. 5), that the ecosystems in the polar regions are vulnerable to shipping. For

this reason, it is important to keep emissions of shipping as low as possible especially in polar waters.

Emissions can be lowered effectively by using less fuel. Using less fuel in every day operation means also cost savings for the ship owner. The running costs of the ship can be reduced which can lead to lower cost of transport to customers or higher profit for the ship owner.

Emissions of new ships are regulated by IMO Energy Efficiency Design Index (EEDI). The EEDI sets a limit value of CO₂ emissions per capacity in tonnes per nautical mile expressed as g/t*nm. EEDI value is calculated for each new ship and the attained EEDI value must be lower than the limit value based on the given reference value. The reference value is reduced in year-based phases and the limit is stricter in every phase. I.e. ship constructed in 2025 must have 30% lower EEDI value whereas a ship constructed in 2023 must have an EEDI of 20% lower compared to a ship built in 2013. (IMO 2010)

Because of the EEDI the emission regulations are becoming stricter in the future. The EEDI value must be lowered in the future to meet the regulations for reducing emissions. The reduction can be i.e. by increasing the capacity of a ship in tonnes or reducing the emissions by using less fuel. With the use of thinner plates, the capacity of the ship can be increased, and the fuel consumption could be reduced because of the reduced weight of the ship. The use of high strength steel could help to meet the emission regulations in the future.

Lower weight and emission reductions could also provide cost savings for the ship owner. The cost savings and lowering of the environmental impact could also be achieved in the manufacturing phase of the ship. Amount of welding needed to construct a ship could be lowered by using lower plate thicknesses. Thinner plates do not require as much welding as thick plates.

Zukauskaitė et al. (2013) found out, welding is a major energy consumption in ship construction. By reducing welding, the amount of energy used in ship construction could be lowered. This would reduce the environmental impact and costs of construction. Zukauskaitė et al. (2013, pp. 177-178) also stated that welding causes health issues of the welding

personnel. By reducing the amount of welding required these health issues could be prevented and the work safety of the personnel could be improved.

1.3 Research objectives

The main objective of this research is to develop a method to design an ice strengthened containership when using high strength steel in the design. High strength steel used in this research has a yield strength of 690 MPa. Hull scantlings can be reduced when using high strength steels as the material can withstand higher stresses. Smaller scantlings in hull structure may increase the cyclic stress in the structural members because higher stresses can be allowed.

Second objective of this study is to solve possible fatigue related issues in the design method. Focus of this part is mainly on the design phase of shipbuilding process by focusing on the different detail geometries. Details that are considered in the research are end connections of longitudinal stiffeners. Welding and post-welding treatments are considered by numerical assumptions. The welding procedure and post-welding treatments can significantly affect the fatigue strength of a connection.

1.4 Research problem and research questions

The research problem is that there are no container ships designed from steel with a minimum yield strength of 690 MPa before, so there is no knowledge of how to conduct such a design. The use of higher strength steel is expected to lead to fatigue problems. These fatigue issues need to be solved in order to utilize the possible benefits of high strength steel on ships weight

The research questions are presented below.

1. How to design longitudinal strength of an ice strengthened container ship when using high strength steel as a construction material?
2. Will the use of high strength steel lead to fatigue issues?
3. Is there weight savings to be achieved by using high strength steels in design?

These research questions are answered using the methods described in Chapter 3. The results obtained are presented in Chapter 4. Finally, the results are analyzed and discussed in Chapter 5.

1.5 Scope of research

The research focuses on designing longitudinal structure of a container ship parallel midbody. The container ship used as an example ship in this study will have a capacity around 15000 TEU. TEU stands for twenty-foot equivalent unit which has the same dimensions than a twenty-foot freight container. It is a common measure used to describe the container capacity of a vessel. One twenty-foot freight container has a length of 6,1 m, width 2,44 m and can have a height from 2,44 m to 2,59 m. (ISO 668 2013, p. 5.) The ship is estimated to have an overall length of around 400 m.

Midship section scantlings are designed against global loading in this research. This means that the scantlings are determined so that they can withstand global bending moments acting on the hull. Moments that are considered in the study are still water bending moment and vertical wave bending moments. Ice strengthening on the midship section is obtained from Aker Arctic Technology calculations and are designed to ice class PC-3.

Bending moments are defined using the LR Rules and Regulations for the Classification of Ships, July 2019, hereinafter referred as the Rules for Ships. Rules for Ships have integrated the requirements of International Association of Classification Societies (IACS) UR-S11A. UR-S11A is a longitudinal strength standard for container ships published by IACS in 2015. The rule-based approach gives a reasonable bending moment values to determine cyclic stresses, as the hull scantlings need to comply with the rule requirements even if the actual calculated bending moment would be lower. The rule bending moments are dependent on the ship's main dimensions. The UR-S11A offers detailed calculation for container ships.

The fatigue assessment focuses on end connections of longitudinal stiffeners when determining fatigue issues of the designed midship section. These are locations where a longitudinal stiffener or a frame connects to a transverse structure. The connection acts as a stress riser in the structure and has higher stresses than a smooth part of the longitudinal structure. As the study focuses on longitudinal structure, transverse structure is not examined

in this study other than for the longitudinal end connection of a longitudinal stiffener or a frame. These locations are confirmed by a literature study and used in finite element modelling.

1.5.1 Exclusions in the research

As a part of the scope of research this paragraph describes everything that are excluded from the research. Exclusions in the study are made for research purposes to narrow the study and to keep the focus of the study in the main objectives. Excluded subjects described are still important aspects to consider when designing a ship that will be built. Subjects that are excluded from the study would need further research before the full possibilities of steel with 690 MPa yield strength could be utilized in design. Excluded items are listed in Table 2.

Table 2. Excluded items

Loads:	Structural details:	Environmental conditions:	Other items:
Loads from containers	Bow region	Ship ice interaction	Manufacturing
Ice loads	Stern region	Temperatures below -10 °C	Ship types other than container ships
Hydrostatic loads	Transverse structures	Water temperatures below 0 °C	Ships with uncommon shape and structure.
Hydrodynamic loads	Hatch covers		Fatigue at load ranges below fatigue threshold.
Whipping loads			
Springing loads			
Bow flare			
Torsion loads			
Horizontal global loads			

Local loads are not considered when determining the fatigue life and cyclic stress. Local loads can be induced by i.e. hydrostatic ballast water pressure against ballast tank's walls or sloshing and dynamic loads of a liquid cargo. These local loads are dependent on the tank plan and general arrangement of a specific ship. Local loads due to container lashing are not taken into consideration in the research. Local pressures are only considered when dimensioning scantlings for the two midship sections, loads due to lashing are not included in the scantling determination. Required scantlings are calculated according to the Rules for Ships using RulesCalc software. Local loads are not studied any further as the study focuses on global loading. Local scantling requirements are checked in order to produce a realistic midship section.

The study is made with an example containership with a capacity of 15000 TEU. Other ship types are not considered in the study. The ship's estimated rule length of 380 m is based on existing ships. Other main dimensions will be selected based on the existing ships with the same length and TEU capacity as the example vessel used in the study.

Due to the large size of the vessel, whipping and springing effects are acting on the ship's hull. Whipping is described to be large flexing of the ship's hull that is originated from the wave impacts of the ship. Vibration of the ship's hull that happens on the resonant frequency is called springing. The springing effect is caused by the frequency of the wave encounters. (Lloyd's Register 2018, pp. 9-10.) Both whipping and springing phenomena are excluded from the study as they are time consuming to analyze and would require specific software to calculate. Also, the effects of bow flare are excluded from the study as the bow shape is not known.

Part of the ship that is under research is the parallel midship section. This includes three container holds separated by a transverse bulkhead. Structural response and designing of the transverse bulkheads are not studied. Other structural locations related to container handling are not included in the study. These locations are i.e. hatch covers and lashing bridges. Transverse structures are not included in the study.

Loading of the ships will only include global bending moments. These include still water bending moment and vertical wave bending moment. The still water bending moment is

assumed to be stay constant in the study. Container ships are assumed to carry fixed number of containers all the time, as some containers will be unloaded and some loaded when the ship calls port. Fuel consumption of the ship would change the still water bending moment of the ship in real life, but the change is assumed to be small and is excluded from the study. The assumption of constant still water bending moment is also made to simplify the comparison of fatigue lives.

Vertical wave bending moment and torsional moments would require detailed modelling and numerical analysis of the ship. As the hull form and layout of the ship is not known, the modelling cannot be made with required accuracy. 4R method currently supports only uniaxial loading. Because of this torsional and horizontal loading are excluded from the fatigue assessment.

Ice loads from ship-ice interaction are not considered when defining the fatigue life or hull scantlings. Ship is assumed to operate outside cold air regions. Mean air temperature is assumed to be $-10\text{ }^{\circ}\text{C}$ at the lowest, and lowest mean water temperature $0\text{ }^{\circ}\text{C}$. Lower mean temperatures than the ones mentioned here are excluded from the study.

The research focuses on the structural design phase. The design of manufacturing is not included in the research. Welding is considered for the 4R calculation method, but as the study is not focusing on the weld design the fatigue calculations are made for weld toe only. Weld root fatigue is excluded from the study as the effect of using high strength steel as base material is studied. Welding and post-welding treatments are crucial parts of improving fatigue life and they are considered as ways of how fatigue life could be improved if needed.

In the fatigue assessment the research focuses on tensile-tensile fatigue or tensile-compression fatigue. Compression-compression fatigue is not included in the study. It is assumed that no fatigue failure happens in compression-compression loading and when stress range is below calculated fatigue threshold value.

1.6 Hypothesis

As a hypothesis it is expected that the design of a container ship using high strength steel can be done in the first place. It is expected that high strength steel could be used in the

design similarly than thick plates are now used. It is expected that the allowable stress can be increased when using high strength steel and therefore smaller plate thicknesses could be used.

Currently the bending induced stresses are kept under the rule maximum allowable stress by increasing the thickness of a member when moving away from the ship's cross sections bending stress neutral axis. Stresses due to global bending moments increase when moving further away from the neutral axis. This is already done to extent of steel with minimum yield strength of 460 MPa according to Rules for Ships (Lloyd's Register 2019, p. 176).

Fatigue issues are expected as the allowable stress in a member is increased. The allowable cyclic stress increases the same time as the allowable static stress increases. The critical fatigue stress range of the material does not increase as the yield strength increases. It is expected that the stress range will increase above the critical stress range of the material in welded joints, as the welded joints act as stress risers in the structure. It is expected that these fatigue issues can be solved by using a joint type that does not create such high stress concentration or by using post-welding treatments that lower the weld-induced residual stresses in the joint.

Overall, it is expected that the use of high strength steel will bring notable weight savings in an ice strengthened container ship. Notable amount of weight saving is expected to be achieved in the main deck and hatch coaming structure. Currently relatively thick plates are used in the main deck to compensate the large deck openings for container holds. These thick plates are expected to be replaced by thinner plates made from high strength steel.

2 PRINCIPLES OF GLOBAL LOADS AND CRITICAL LOCATIONS IN CONTAINER SHIP CONSTRUCTION

This chapter focuses on studying existing literature and previous research about ship's longitudinal design and high strength steels in ship building. Aim is to study the design process of container ships in order to the design withstand global hull girder loads. This is important knowledge for the study, as the high strength steel will be implemented into the design of a case ship.

This chapter also studies the fatigue issues related to ships. Aim is to identify critical locations in container ship's prismatic midbody that are prone to fatigue. These findings are then used as a basis for critical locations as described in Section 3.6.

2.1 Design principles of ship structural design

The basic principles of structural design apply to longitudinal strength design as it is a part of the ship design process. Design methods of a ship can be divided into three basic categories as stated by Bai and Wei-Liang (2015, p. 3). The three categories are: design by the rules, design by analysis and design based on performance standards. Also, the two main design principles are reliability-based method or parametric design and rationally-based method (Hughes & Paik 2010, Ch. 1, p. 2).

Defining the loads acting on the ship's hull are important part of the strength design process. The loads and the reasons behind them are described separately in Section 2.2. Calculation of the longitudinal loads in the study are described in Section 3.3.

2.1.1 Reliability-based design

Usually ships are still designed according to the rules of classifications societies. The rules provide a simple, equation-based way of determining loads acting on the ship's hull. Time savings can be accomplished in the design when using the load definitions from the rules, as there is no need to compute the loads with a 3D simulation tools. (Hughes & Paik 2010, Ch. 5, p. 31.) The given load values in the rules are also the same values that are needed to be

used in the design in order for the ship to comply with the rules and get a class approval (IACS 2019a, p. 18).

The rule-based design is a parametric design approach. The values for i.e. bending moments and stresses are linked to the main dimensions of the ship. The parametric design is a useful tool in the preliminary design of a ship, also including the strength design. Further in the design process, a design based on simulations can be utilized. (Lamb 2003, Ch. 11, p. 4.)

The design by rules includes a method called limit-state design. In the limit-state design every structural component is checked against limit values of different failure modes. The limit states are usually categorized into four limit states. These states are serviceability limit-state (SLS), ultimate limit-state (ULS), fatigue limit-state (FLS) and accidental limit state (ALS). In practice, a limit value of stress is calculated for each limit state and the lowest limit state value is driving the design. (IACS 2019a, p. 29; Bai & Wei-Liang 2015, pp. 3-5.)

Bai & Wei-Liang (2015, p. 5) provided an example that, if critical buckling stress value (ULS) is lower than the value of static membrane stress value for yielding (SLS), the critical buckling stress value is driving the design. The design is to be made so that the stress value in the member needs to be lower than the limit value, or the limit value needs to be increased i.e. by increasing the material strength or geometry. This is expressed by equation 1 (Bai & Wei-Liang 2015, p. 5).

$$S_d \leq R_d \quad (1)$$

where:

$S_d = \sum S_k \cdot \gamma_f$, Design load effect

$R_d = \sum R_k / \gamma_m$, Design resistance or capacity

S_k = Characteristic load effect

R_k = Characteristic resistance

γ_f = Load factor that is reflecting the uncertainty of the load

γ_m = Material factor that can be expressed as inverse resistance factor

The equation presented above represents Load and Resistance Factored Design (LRFD) that can also be called as Partial Safety Factor method (PSF). As the name says, it utilizes safety factors to take the uncertainties of the calculations into account in the design. The Common Structural Rules (CSR) (IACS 2019a) utilizes PSF to determine the hull girder ultimate limit-state (ULS). The CSR is a rule set created for designing oil tankers and bulk carriers. It is widely known in the shipbuilding industry and noted by classification societies. In SLS, FLS and ALS the CSR utilizes a method called Working Stress Method (WSM).

The WSM method is also called as allowable stress method. Difference to PSF is, that the WSM uses one safety factor instead of two. One safety factor includes the uncertainties of both the load and resistance, whereas the PSF has individual safety factors for both. By utilizing safety factor, it reduces the allowable stress limit to be below the ultimate resistance capacity of the structure. (IACS 2019a, p. 31; Bai & Wei-Liang 2015, p. 4.)

Design of a hull girder is made using PSF as described above. The failure modes of structural members are defined so the limit state values can be calculated based on the first principles of engineering (Hughes & Paik 2010, Ch.5, p. 36). In addition to Hughes and Paik, the CSR also states that the SLS and ULS limit states are to be satisfied for hull girder.

In order to comply with the limit state criteria, the stresses acting in the structural member are to be less or equal at maximum of the limit stress value. This is expressed in the CSR for the hull girder yielding (SLS) as described in equation 2. (IACS 2019a, p. 328.)

$$\sigma_L = \sigma_{perm} \quad (2)$$

where:

σ_L = Normal stress

σ_{perm} = Permissible hull girder bending stress

Normal stress acting in the member are derived from the vertical bending moments. A safety factor is added to the normal stress calculation in the CSR to represent the non-uniform distribution of ship heading when the ship is in seagoing condition. In the criteria it is assumed that the ship is in intact condition, so there is no flooding of the ship. (IACS 2019b, Ch. 5, Sec. 1, p. 4.)

2.1.2 Rationally-based design

Another design method is presented by Hughes & Paik (2010, Ch.1, pp. 1-3) to be used instead of reliability-based parametric method. This method is called rationally-based structural design. The rationally-based structural design relies on the mathematical capabilities of computers and 3D modelling. In the rationally-based design, the loads and structural responses are calculated directly with a help of finite element analysis (FEA) and hydrostatic or hydrodynamic modelling. This leads to far more precise calculations in both fields. The structure's capacity can be utilized far better than with the use of prescriptive equations, as the uncertainties do not have to be considered by using safety factors that may lead to overly designed structure. The rationally-based method uses numerical methods instead of the prescriptive set of equations based on the first engineering principles or the rule-based equations which tend to have experience-based correction factors added to the first engineering principles.

The rationally-based method described by Hughes and Paik (2010, Ch.1, pp. 1-3) typically provides more precise results than the reliability-based method. Calculation process is on the other hand much more time consuming and require computing power and tools. Also, the rationally-based design method is reliable and accurate if all the possible load cases are known and considered.

As the ship in the study is an example ship with only a midship section and main dimensions all the loads are not known. For this reason, the rationally-based methods are not utilized in all cases in this study. The rationally-based methods are used when stress concentration factors are determined for the fatigue life analysis.

2.2 Longitudinal loads acting on the ship's hull

The global loads that act against the ship's hull are described in this part. The loads considered in this study are described in Section 1.5. Loads that are excluded of the research are described in Subsection 1.5.1.

For longitudinal strength, a ship is usually idealized as a beam. By assuming the ship to act as a beam, equations and calculation methods for structural beams can be utilized. Ships are naturally slender as they are long compared to their cross-sectional area. The Bernoulli-Euler

simple beam theory has been used in ship design already in 1988 by assuming that a ship acts like a beam under loading. Studies made after the introduction of the theory found out that the Bernoulli-Euler beam theory gives accurate results for a ship structure. (Edward 1988, p. 235.) The same assumption is still in use in the CSR and in UR-S11A (IACS 2019b, Pt. 1, Ch. 3, Sec. 5 p. 3).

The hogging and sagging conditions can also occur due the loading of the ship in still water condition. Hogging or sagging can be a result of a loading of the ship where the parallel midship section has different weight and buoyancy than the bow and stern. In hogging condition, the ends of the ship bend downwards. On the contrary in the sagging condition, the ship's ends are bent upwards. Still water hogging and sagging are shown in Figure 1.

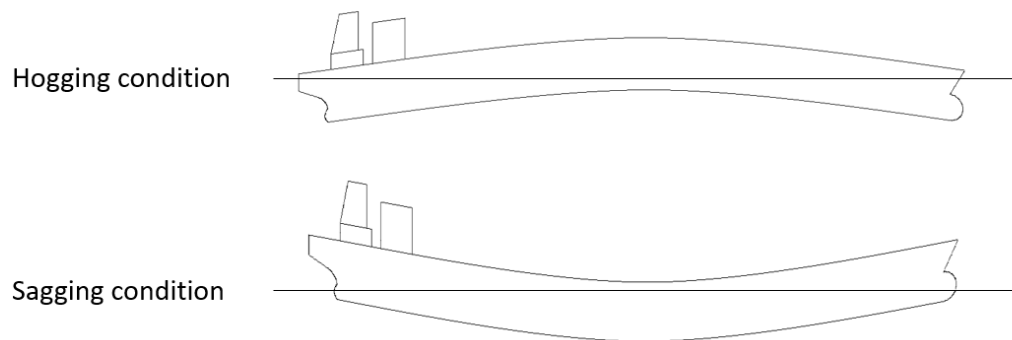


Figure 1. Hogging and sagging conditions in still water.

The ship's hull girder loads can be defined according to the Bernoulli-Euler simple beam theory. Ship is idealized as a beam that is affected by shear forces. These shear forces induce bending moments in the idealized ship beam. These loads originate from the environment that the ship is operating in. They can be considered as independent from the internal structural layout of the ship and be more related to weight distribution of the ship. Hull form is linked closely to environmental loads that the ships is subjected to. (Hughes & Paik 2010, pp. 9-11.)

The loads described above can be classified into two different loads: static and dynamic loading of the ship. The static loading refers to so called still water bending moment and

dynamic loading to wave bending moments. (Mansour & Liu 2008, Section 2, p. 4-5.) The same separation of loads is made by Hughes and Paik (2010, Ch. 2, pp. 2-4). They divide the global loads into static and slowly varying loads. The static loads are defined similarly in both definitions as well as the low-frequency or slowly varying loads despite the term to describe the loads is different.

2.2.1 Still water bending moment

According to Mansour and Liu (2008, pp. 4-6) the still water bending moment can be divided into gravitational force and buoyancy force. The buoyancy force can be described as resultant of hydrostatic pressure acting against the ship's hull that is under water. This buoyancy force always acts upwards to the opposite direction than gravitational acceleration. Buoyancy b pressure can be taken as shown in the equation 3. (Mansour & Liu 2008, p. 5.)

$$b = \rho g A \quad (3)$$

where:

ρ = Density of water kg/m^3

g = Gravitational acceleration m/s^2

A = Immersed area m^2

Similarly, the weight of a ship can be described as weight per unit length. The weights in the ship consists of hull steel, cargo, ballast, machinery etc. Everything that is carried on board the ship is included in the weights of the ship. These weights are distributed over the entire length of the ship. These weights are dependent on the configuration and layout of a specific ship. (Mansour & Liu 2008, p. 5.)

These two forces are acting simultaneously every time the ship is afloat according to Archimedes' principle, they cause a bending moment to the ship. The bending moment can be derived simply by computing a double integral over the sum of total buoyancy and total weight force acting on the ship's hull (Hughes & Paik 2010, Ch 3, p. 2). Same computation is described by Mansour & Liu (2008, p. 7) by first computing the shear forces $V(x)$ acting over the length of the ship. The shear force is described in equation 4.

$$V(x_1) = \int_0^{x_1} [b(x) - w(x)] dx \quad (4)$$

where:

$b(x)$ = buoyancy per unit length

$w(x)$ = weight per unit length

The still water bending moment $M(x_1)$ acting on the ship's hull in certain location can be computed from the shear force by integrating the calculated shear force over the length of the ship. The still water bending moment can be calculated as in equation 5. (Mansour & Liu 2008, p. 7.)

$$M(x_1) = \int_0^{x_1} V(x) dx \quad (5)$$

The minimum still water bending moment to be used in design is usually computed in the rules as a simple equation. As stated by Manson & Liu (2008, p. 7) typically the still water bending moment acting on the ship is on the other hand calculated with a help of a computer software. The “rule-based” design is still a time saving tool in preliminary design phase of a ship when the complete layout is not yet designed.

The CSR presents a simple equation for determining the minimum design still water bending moment of a vessel. The minimum still water bending moment is derived for hogging and sagging situations separately. (IACS 2019a, p. 183.) The equation for hogging situation is presented in equation 6.

$$M_{sw-h-min} = f_{sw} (171 C_w L^2 B (C_b + 0.7) 10^{-3} - M_{wv-h-mid}) \quad (6)$$

where:

f_{sw} = Distribution factor along the ships length as described in the CSR (IACS 2019a, p. 183)

C_w = Wave coefficient

L = Rule length

B = Molded breath

C_b = Block coefficient

$M_{wv-h-mid}$ = Vertical wave bending moment, hogging

The still water bending moment is described as a function of the ship's main dimensions. The minimum still water bending moment is not directly linked to the hull form of the ship and can then be calculated before the complete hull form is known. The value of moment obtained using the equation 6 is the minimum still water bending moment that the ship must withstand.

CSR also presents a similar equation for sagging situation. UR-S11A describes the still water bending moment to be calculated for all loading conditions of the ship separately. This can be done by using the equations 4 and 5 or by using a dedicated software to calculate still water bending moment.

Typical still water bending moment distribution along the ship's length in loaded condition is shown in Figure 2. The shear force and weight distribution are shown alongside the still water bending moment distribution. The Figure 2 describes a still water hogging situation. In the Figure 2, the curve 1 represents the bending moment M . In the shown condition the M has positive values. This means that as the ship is in hogging condition, the structures above the neutral axis like main deck structures are in tension. On the contrary, the parts under the neutral axis like bottom structures are in compression.

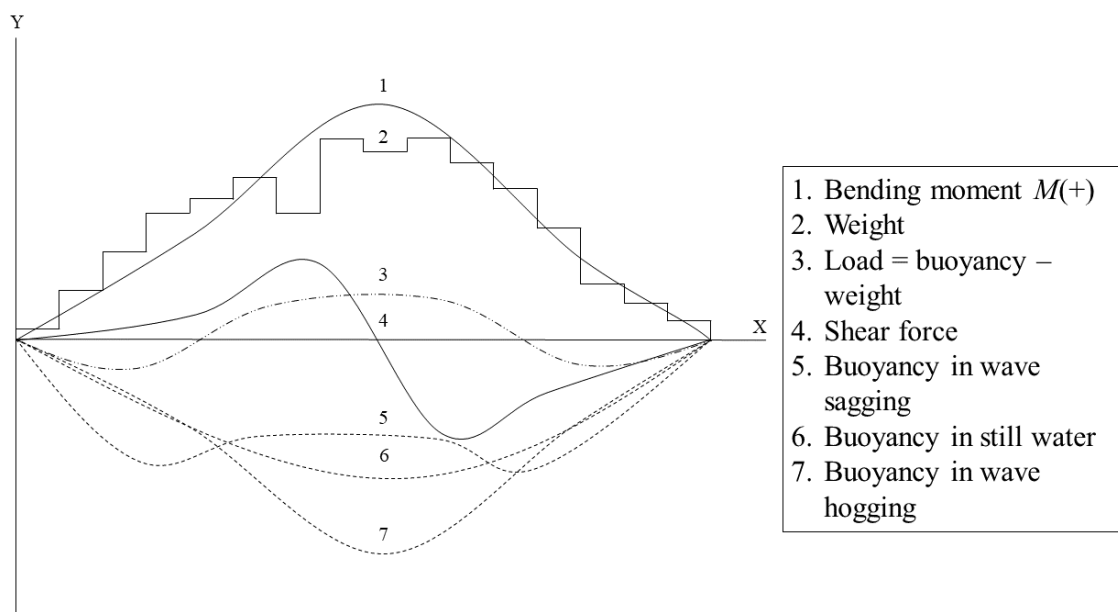


Figure 2. Forces and bending moment acting over the ship's length (mod. Mansour & Liu 2008, p. 7).

The curves 5 and 7 in Figure 2 relate to hogging and sagging conditions due to wave encounters. The wave hogging and sagging are described in subchapter 2.2.2. The wave sagging and hogging conditions are shown in Figure 3 in subchapter 2.2.2.

The values of still water bending moment are related to the loading and dimensions of an individual ship. Numerical values are quite large due to the large size and capacity of a ship, i.e. the maximum still water bending moment of a 302 m long container ship is around $6.1E+06$ kNm (Committee on Large Container Ship Safety 2013, p. 9,42).

2.2.2 Wave bending moments

The second category of loads are described as quasi-static loads, low-frequency loads or wave induced loads. When a ship encounters a wave, the area of the wetted surface changes compared to situation where the ship floats in calm conditions. This results to a changed pressure distribution on the ship's shell and changes the buoyancy force distribution. Now the buoyancy force is distributed differently compared to the static equilibrium in still water condition. The resultant of downward and upward forces induces a moment to the ship's hull different from the still water bending moment, which is called wave bending moment. (Lamb 2003, Ch. 18, pp. 8-9.)

The bending moments due to wave encounters are described in the CSR similarly to the still water bending moment. The wave bending moments for hogging and sagging situations are described separately. The equations are linked to ship's main dimensions as in still water bending moment derivation. (IACS 2019a, p. 187.)

Terms sagging and hogging can also be related to a wave encounter of a ship. The terms are linked to a theoretical situation where the ship encounters a wave with same wavelength as the ship's length. (Molland 2008, pp. 672-674.) In hogging condition the ship is placed on top of a wave resulting the ship's ends to bend downwards. On the contrary, in sagging condition, the ship is placed to the crest between two waves, resulting the ship's ends to bend upwards. Wave hogging and sagging conditions are shown in Figure 3.

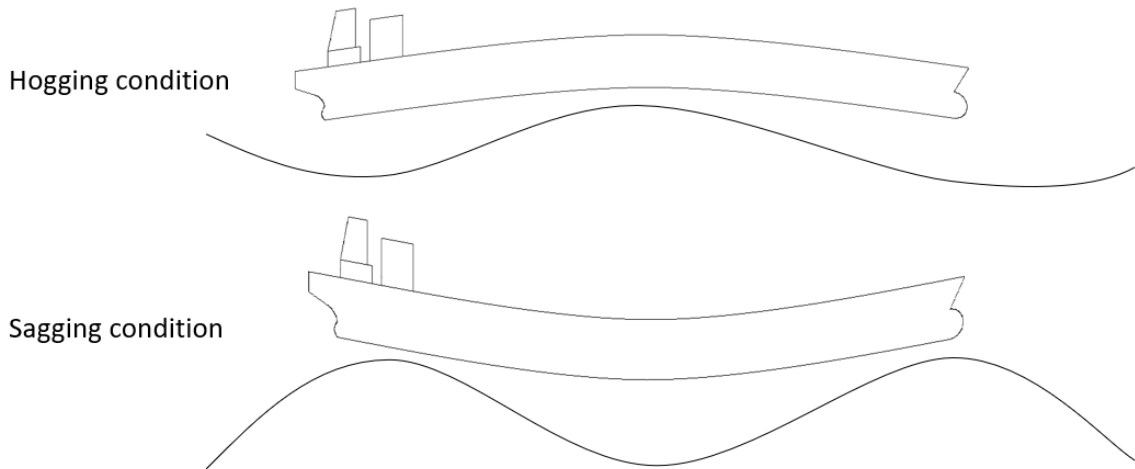


Figure 3. Ship placement in waves in wave sagging and hogging conditions (Molland 2008, p. 674).

IACS describes in the UR-S11A the wave bending moments for container ships in a similar way as the CSR for oil tankers and bulk carriers. As this study is focused on container ships, the UR-S11A wave load determination is more suitable than CSR. The used wave bending moments are described in Subsections 3.3.2.

A difference to the still water bending moment is that hogging condition is assumed to be linear in the CSR, but sagging is not. For this reason, a non-linear correction factor f_{NL} is implemented into the rule wave bending moment calculation. This factor is dependent on the ratio between sagging and hogging moments. (IACS 2019b, Pt.1, Ch.4, Sec.4, p. 4.)

The equation-based wave load design described above is based on the most severe wave that the ship is likely to encounter. This method is called the design wave method. The design wave method is used to determine the response of the structure when encountering a wave and this calculated response is used to design the ship. The ship is expected to encounter a large wave with a probability of exceedance of 10^{-8} during the lifetime of the ship. This value is determined based on the measured wave data on the North Atlantic when the ship is expected to operate for 20 years. (Bai & Wei-Liang 2016, p. 89.)

The same probability of exceedance is assumed in the CSR for the strength assessment but assumed to be 10^{-2} for a reduced design wave in the fatigue assessment (IACS 2019a, p. 159). The CSR utilizes a wave coefficient C_w in wave load calculation. This wave coefficient

is based on the wave statistics of North Atlantic as stated by Bai and Wei-Liang (2016, Ch. 5, p. 89). The CSR also uses an adjustment factor f_p wave-induced loads, that implies the probability of exceedance on 10^{-8} in the strength assessment. (IACS 2019b, Pt. 1, Ch. 4, p. 1.)

Bai and Wei-Liang (2016, pp. 172-173) also represents another method of determining wave-induced loads than the design wave method. More sophisticated method for determining wave loads for ships is to model the ship in a computer software. The software calculates the hull response for different wave encounters considering the variation in wave height and direction. This analysis gives more accurate results than the design wave method but is more time consuming as the hull response is calculated for each wave encounter. The analysis is time dependent numerical analysis that is done by a computer code. These numerical calculation methods are sometimes called as spectral analyses as in Lloyd's Register FDA – Application and Notations (Lloyd's Register 2017, p. 7).

As an example, Lloyd's Register utilizes ShipRight software in LR Fatigue design assessment. A full spectral analysis is made based on the principle methods to determine the stresses acting in hull structure due to wave encounters. The analysis made in ShipRight includes the effects of hydrodynamic loads and ship motions combined to a finite element analysis (Lloyd's Register 2017, p. 29).

2.3 Steel grade in strength design

Yield strength of the selected steel is a part of the calculation process to determine the permissible hull girder bending stress of a structural member in the parametric design approach in the CSR. The steel grade affects the permissible hull girder bending stresses as well as the minimum value for vertical hull girder net section modulus, which affects the normal stress in the structural member. (IACS 2019a, p. 329.)

The steel grade is considered by a material factor k . This material factor is dependent on the yield strength of used structural steel. In this study the material factor is noted as k_L . The material factors for steels with different minimum yield stresses are presented in Table 3.

Table 3. Material factor according to IACS (UR-S4 2010, p. 82).

R_{eh} , specified minimum yield stress in N/mm ²	k_L
235	1.00
315	0.78
355	0.72
390	0.68

The origin of the material factor refers to a unified requirement published by IACS in 2010. The unified requirement defines the material factor similarly based on the yield strength of used steel, but no equation is presented for computing a k_L factor for steels that have higher minimum yield stress than 390 N/mm². (UR-S4 2010, p. 1)

LR presents a similar table for material factor (higher tensile steel factor k_L) with an exception of determining a value for steel with yield strength of 460 N/mm² to be 0.62. The steel with yield strength of 460 MPa is referred hereinafter as AH47. Like the CSR, LR does not specify a way of determining k_L factor values for steels with higher minimum yield strength than specified in the Rules. (Lloyd's Register 2019, pp. 176-177.)

The higher tensile steel material factor k_L takes corrosion into account as well as the material yield strength. The material used in the hull construction is expected to corrode during service. The absolute amount of the material that is allowed to corrode is the same for every material. For thinner plates, the allowed amount of corroded material is relatively larger than for a thick plate. E.g. if 2 mm corrodes from an originally 4 mm thick plate, the corroded amount is 50% of the original thickness. Similarly, if the same 2 mm corrodes from a 20 mm plate, the corroded amount is 10% of original thickness. (Hong 2019.)

For mild steel with yield strength of 235 MPa where thicker plates are expected to be used, the section modulus should be at least 90% of the original after the corrosion. For steel with yield strength of 355 MPa the amount of section modulus is to be at least 83% of the original value. For steel with yield strength of 690 MPa, hereinafter referred as AH70, the amount of section modulus after corrosion can be assumed to be at least 58% of the original. Using these assumptions, the k_L factor can be taken as 0.53. (Hong 2019.)

2.4 Critical fatigue locations in container ship midship section

Due to the increase in container ship sizes, steels with high minimum yield strengths are being used in construction. As the high strength materials provide higher static capacity of the material, the cyclic stresses are also increasing. Also, the fatigue strength of a weld or a base material is not necessarily increased while the material yield strength increases.

Even when using steels with minimum yield strength up to 460 MPa, thick panels must be used in deck structures of a container ship. These thick plates lower the fatigue capacity even more due to the thickness effect. (Li et al. 2014, p. 65.) According to DNVGL-CG-0129 (2018, pp. 41-46), the thickness effect is due to the small weld geometry size compared to the geometry size of the plates around the weld. Thickness effect is also recognized by IACS (2019a, pp. 545-546). According to the CSR part 3.3.1 the thickness effect affects the stress distribution through the thickness of a plate or a component where the crack propagates. The CSR uses a correction factor to include the thickness effect into the calculations.

Fatigue failure needs a crack propagation to happen for the fatigue crack growth to start. As noted by Li et al. (2014, p. 65) in container ships thick plates usually used in structures close to main deck. These thick panels are needed to satisfy the longitudinal strength of the ship, as the container holds create large openings to the deck. Any crack i.e. crack due to brittle fracture or manufacturing error defect in the panel can be a possible location of fatigue failure. The cyclic loading can lead to crack growth and finally fatigue failure in a structural member. (Sumi et al. 2013, p. 496.)

One of the critical locations for a fatigue crack in a container ship structure is a longitudinal weld in a hatch coaming, which is a specific structure for container ships. This is due to the high plate thickness in the hatch coaming and because the hatch coaming is subjected to the highest longitudinal bending stress and therefore also to highest hull girder stress ratio. (Sumi et al. 2013, p. 501.)

LR presents Fatigue Design Assessment (FDA) Level 1 procedure Structural Detail Design Guide (SDDG) where the locations that LR has identified based on their analyses and service experience to be critical. The critical locations identified for containerships are described to have high stress variations and concentrations during the ship's operational lifetime. LR also

presents suggestions to improve fatigue performance of critical locations. (Lloyd's Register 2009, p. 99.)

Figure 4 shows the critical locations identified in the SDDG. The first image presents the critical locations in a transverse midship section. The figure also presents location for possible misalignments in manufacturing. For this study, the areas for high stress concentrations are of more interest as the research focuses on design phase.

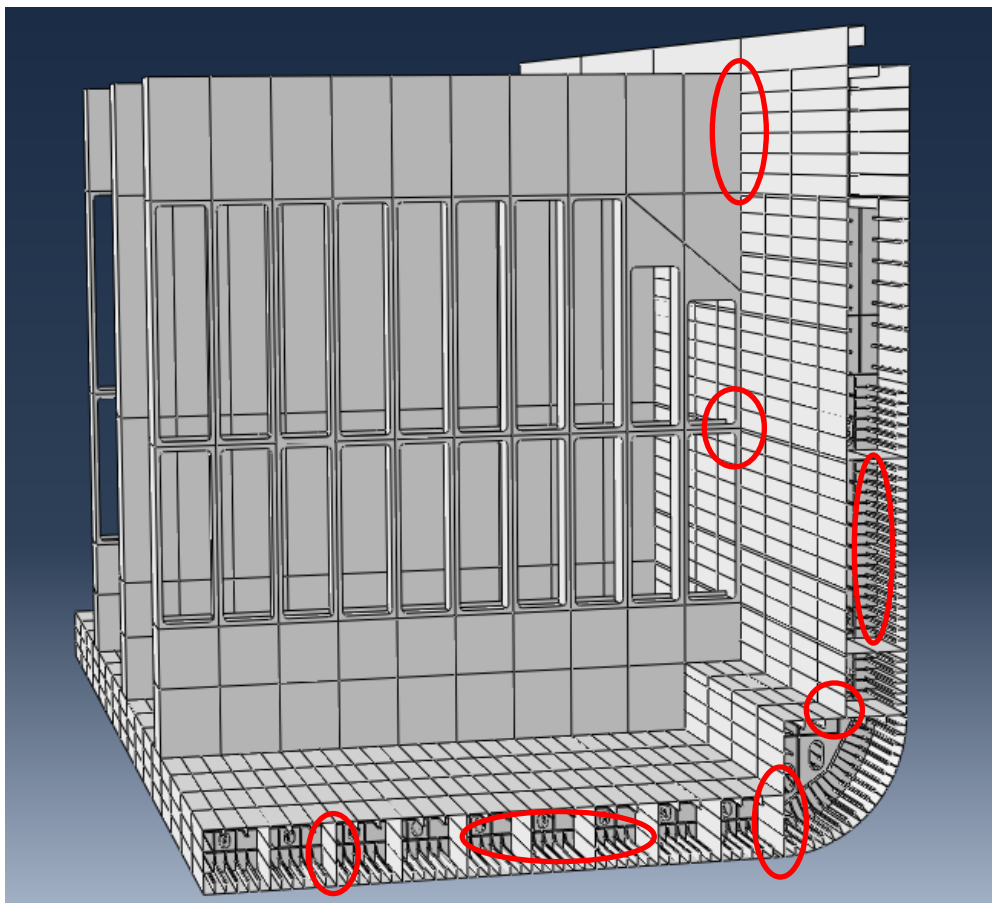


Figure 4. Areas of high stress concentrations (Lloyd's Register 2009, p. 105-108).

IACS Guidelines for Surveys, Assessment and Repair of Hull Structures is a document created to assist IACS member societies in their survey work. The IACS guidelines identify locations where damages have been noticed. The guideline identifies areas that may likely have damages and therefore are to be surveyed carefully. (IACS 2017, p. 4.)

The same locations are advised for the surveyors to give special attention to. Those locations have high possibility to fractures. For deck structures it is advised to give special attention to hatch corners, deck strip plating and weldments and connections related to the hatch coaming structures. For side structures IACS advises to pay special attention to connections between the deck and side longitudinals to a transverse web frame and connections between side longitudinals and a watertight bulkhead. (IACS 2017, p. 25,57.)

IACS (2017, p. 16) presents a detailed guide of the possible fracture locations. Multiple locations throughout the length of the ship are presented. Most of the locations are the same locations as presented by LR (2009, pp. 105-108). As noted by IACS (2017, p. 66) in the Note 1. the damage can be caused by a stress concentration which can lead to a lowered fatigue life in the area.

2.5 Possible fatigue issues when moving to high strength steels

A traditional approach to fatigue life is a S-N curve. S-N curve is also called a stress-life curve. The S-N curve presents the test results of a specific material where a test specimen is subjected to different stress range levels and loaded repeatedly until failure. The curve shows a point where the material is expected to fail under applied stress range of number of cycles applied. S-N curves are usually plotted on a logarithmic scale. (Dowling et al. 2013, pp. 422-423.) An example of a S-N curve for shipbuilding steel with yield strength of 420 MPa is shown in Figure 5.

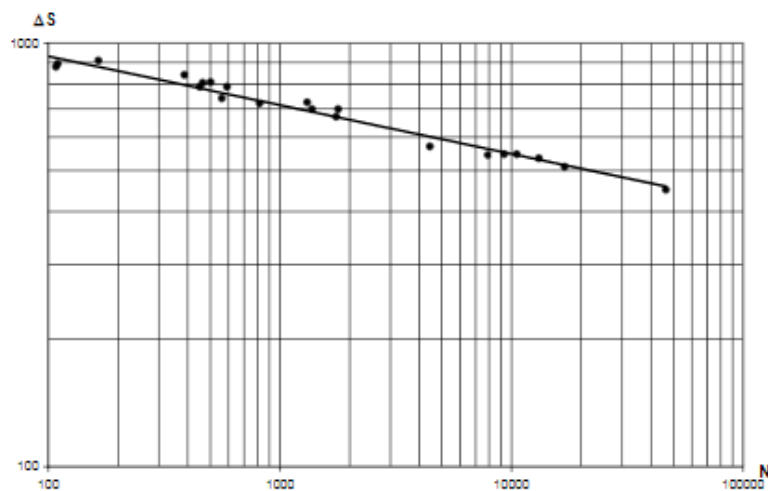


Figure 5. Example of a S-N curve for shipbuilding steel (Parmentier & Huther 2013, p. 51).

As seen from the S-N curve in Figure 5 that by increasing the applied stress amplitude, the needed cycles to failure decreases. Even if the ship could be designed to withstand global static loading, the cyclic loading due to wave environment can lead to failure. With the use of high strength steel, a lower high tensile steel factor k_L can be utilized according to LR (2019, p. 176) and IACS (2010, p. 1). Permissible stress for hull girder bending stress σ_{perm} according to equation 7 (Lloyd's Register 2019, p. 224).

$$\sigma_{perm} = \frac{175}{k_L} \quad (7)$$

As can be seen from equation 7, higher permissible stress can be allowed when using lower k_L factor. Increasing the steels strength and lowering the k_L factor can increase the stress range applied to the structural member by allowing higher stresses in tension and compression when the ship is in hogging or in sagging conditions. By increasing the stress range the needed cycles for failure decrease as seen from Figure 5. If the needed cycles for failure decrease below the cycle of stress ranges that the ship will experience during its lifetime, fatigue becomes a limiting factor for the design.

3 METHODOLOGY

The methodology used in this study is described in this chapter. The methodology follows the rules given in the LR Rules for Ships and IACS UR-S11A for strength assessment and rules given in the CSR for fatigue assessment. The methods utilize a linear finite element model in finding stress concentration factors.

These methods that are described in the chapter are used to give results that answer the research questions described in Section 1.4. Results acquired using these methods are described and analyzed in Chapter 4. The results are further discussed in Chapter 5.

The study follows a flowchart shown on the next page in Figure 6. First part of the design is to determine scantlings on the selected container ship midship section. Scantlings are also selected using high strength steels where it is found to lower the plate thicknesses of scantlings within the limits of the UR-S11A and the Rules for Ships.

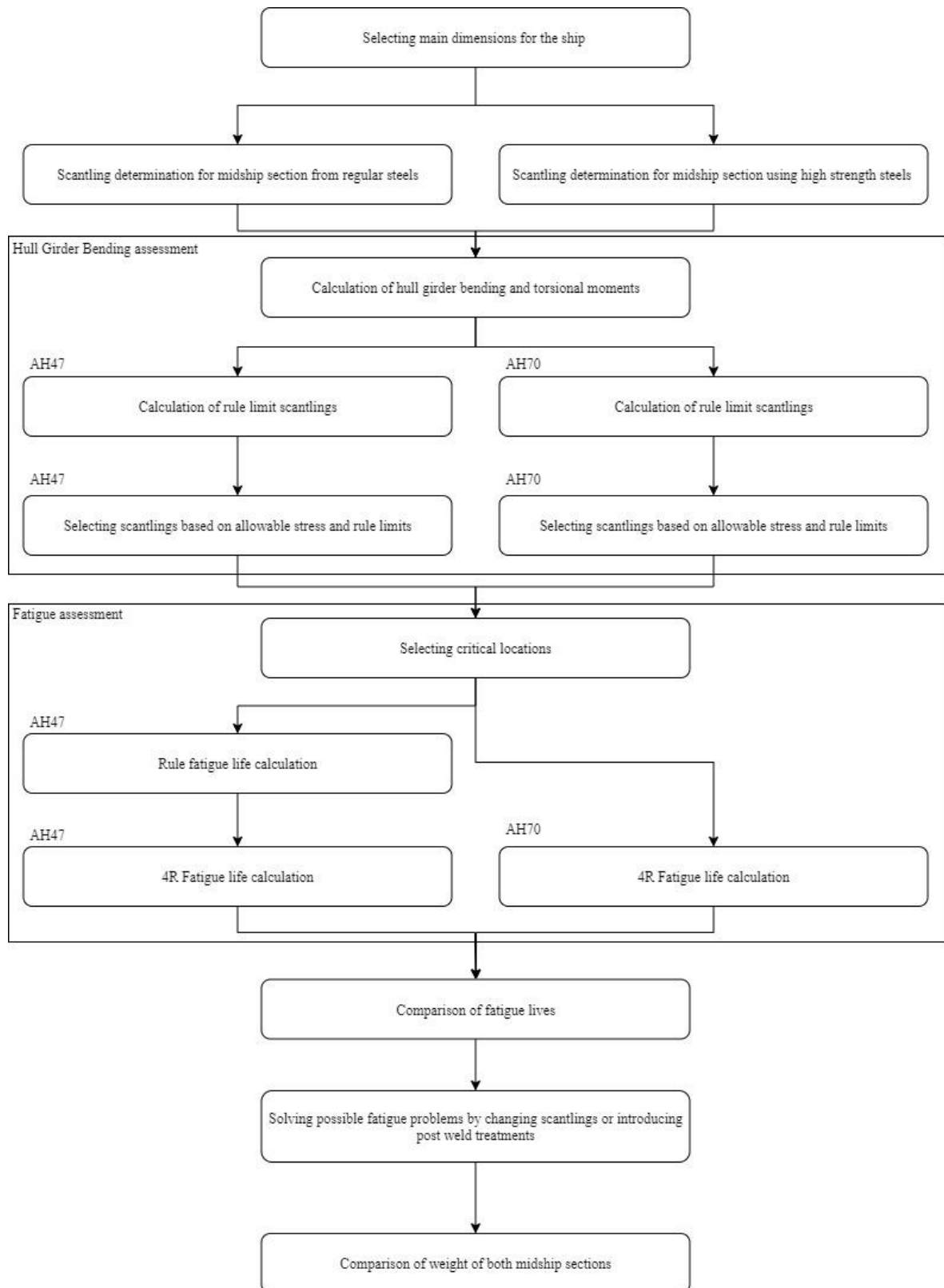


Figure 6. Research flowchart

Second part is to determine the fatigue life for the midship section designed using currently allowed steel grades. The fatigue life is determined using the 4R method, but a rule-based fatigue life is given as a reference to the new 4R method. This is done in order to be able to compare the fatigue lives of the two midship sections, as the rule-based fatigue life assessment cannot be done to the midship section with AH70 steel as it is not recognized by the rules. Finally, the midship section unit weights are compared to see if weight savings could be achieved by using AH70 steel instead of AH47.

3.1 Rule sets and design guides used in the study

In the study three different rules and design standards are used. Two are used for designing scantlings for the midship section. The same rules are used for designing scantlings for midship section with AH47 steel and for midship section with AH70 steel. Additional rule set is used for reference fatigue life calculation.

For scantling design UR-S11A revision 2015 longitudinal strength standard for container ships published by IACS in 2015 is used. The UR-S11A is incorporated into the Lloyd's Register Rules for Ships, Part 4, Ch. 8 Sec. 16. Rules for Ships revision 2019 is also used to calculate local scantling limits. The study is focused on longitudinal strength, so local scantlings are checked using Lloyd's Register software RulesCalc, the use of RulesCalc is described in Section 3.4.

As the UR-S11A does not have fatigue requirements, it cannot be used for reference fatigue life calculations. For rule-based reference fatigue life calculations, the CSR revision 2019 is used. The CSR is a rule set for oil tankers and bulk carriers published by the IACS. The CSR is selected for fatigue life calculations. Although the CSR is not a rule set for containerships, it is commonly known set of rules in the shipbuilding industry and among the classification societies. The study uses fatigue life calculation method called 4R to determine fatigue lives. As the novel 4R method is not commonly known, a familiar fatigue life based on the CSR is presented as a reference point to the novel 4R fatigue life.

3.2 Main dimensions and initial midship section using AH47 steel

Example ship is used as a base of the calculation and design modifications in the research. The example ship is designed to have the maximum capacity of around 15000 TEU. Midship

section layout of the ship is designed by studying existing designs to obtain commonly used general arrangement.

Main dimensions of the ship are selected in an early stage of the study. The same main dimensions are used for both midship section made using AH47 and AH70 steels. The main dimensions are shown in Table 4.

Table 4. Main dimensions.

Rule length	378 m
Moulded breadth	55.4 m
Moulded depth	30.5 m
Summer draught	16.5 m
Scantling draught	16.5 m
Moulded displacement at summer draught	247 800 ton
Block coefficient	0.69
Maximum ahead service speed	23 kn

The midship section layout follows the current practice to have a double skin and a double bottom layout. The double bottom girders are arranged under the container stack corners to carry the weight of the containers. A bilge box and a topside torsion box are designed as they improve the torsion response of the vessel and to increase sectional area. Continuous hatch coaming is used to maximize the use of longitudinal members in midship section modulus at main deck height. The used ordinary midship section is shown in Figure 7. Complete drawing of the initial midship section can be found in the appendix II.

The longitudinal strength assessment is conducted using a LR software RulesCalc. RulesCalc calculates the loads acting on the ship according to the Rules for Ships and UR-S11A for container ships. The equations behind the calculations are obtained from UR-S11A and Rules for Ships and are described in this chapter.

The two limiting factors in the UR-S11A are the hull moment of inertia and permissible hull girder stresses. Midship section is designed so that both requirements are fulfilled. The minimum value of hull moment of inertia I_{net} in m^4 is calculated as in equation 8. The equation in the Rules for Ships is the same that is presented in the UR-S11A (UR-S11A 2015, p. 15).

$$I_{net} \geq 1.55L|M_s + M_w| \cdot 10^{-7} \quad (8)$$

where:

M_s = Still water bending moment in kNm, hogging and sagging

M_w = Design hull vertical wave bending moment in kNm, hogging and sagging

The limit value of hull moment of inertia is applicable both to hogging and sagging conditions. The calculation still water and vertical wave bending moment is described in Subsections 3.2.1 and 3.2.3. In addition to limit hull moment of inertia, the hull girder stresses must be lower than the permissible hull girder stresses.

The permissible hull girder stresses are described in the UR-S11A. The permissible hull girder stresses are to be satisfied when taking still water and wave bending stresses into account. The permissible rule girder stresses σ_{perm} in N/mm^2 are taken according to equation 9 (UR-S11A 2015, p. 14).

$$\sigma_{perm} = \frac{R_{eh}}{\gamma_1 \gamma_2} \quad (9)$$

where:

k_L = Taken as described in Table 3 in subchapter 2.3.

γ_1 = Partial safety factor for material, taken as

$$\gamma_1 = k_L \frac{R_{eH}}{235}$$

γ_2 = Partial safety factor for load combinations, taken as

$$\gamma_2 = 1.24$$

R_{eh} = Yield strength of material

The formulation of higher tensile steel factor k_L is made according to Section 2.3. Based on the assumptions made in Section 2.3, the assumed factor is used in the longitudinal strength calculations. Calculation of the permissible stress can be found in appendices I and II.

3.3.1 Still water bending moment

As there is no final hull form and general arrangement designed for the example ship, the still water bending moment cannot be calculated based on methods described in Subsection 2.2.1. The rule permissible bending moment in the Rules for Ships, Part 3. Ch. 4. Sec. 5.5 is based on the actual hull section modulus. In this research same still water bending moment is used for the two sections, one with AH47 as steel with highest yield strength and one with AH70 to develop comparable designs based on the permissible hull girder stresses.

The still water bending moment is approximated based on still water bending moments of existing container ships. The example ship in this study has a capacity of 15000 TEU. The still water bending moment is linearly interpolated based on two ships, one being smaller and the other being larger by TEU capacity than the example ship in the study.

The smaller ship that is used to determine the still water bending moment is MOL Comfort. MOL Comfort was involved in an accident in 2013 in the Indian Ocean. Due to this a lot of detailed reports and investigations of the ship are publicly available. The ship experienced environmental conditions that caused a fracture to originate from the bottom shell plates. The fracture led to complete loss of integrity of the structure. Finally, the ship's front fell off and drifted away from the remaining stern part. Both parts sank eventually. (Committee on Large Container Ship Safety 2013, pp. 3-4.)

Second ship used as a reference is a 19000 TEU Ultra Large Container Ship (ULCS) designed by Hyundai Heavy Industries (HHI). The ship is presented by Vladimir et al. (2016) to study the direct calculation methods for ULCS structural design. Vladimir et al. (2016)

computed the still water bending moment using direct calculation methods provided by Bureau Veritas.

The main dimensions of both ships are shown in Table 5. The still water bending moments are shown in the table with main dimensions of the vessels. The linear interpolation is made based on the ships' lengths between perpendiculars.

Table 5. Containership comparison (Committee on Large Container Ship Safety 2013, p. 9,42; Vladimir et al. 2016, p. 68,70).

Vessel:	MOL Comfort	HHI ULCS
Length between perpendiculars (L _{pp}):	302 m	383 m
Breadth:	45.6 m	58.6 m
Depth:	25 m	30.5 m
TEU Capacity	8110	19000
Still water bending moment	6.1E+06 kNm	11E+06 kNm

The still water bending moment based on the values presented in Table 5 is shown in subchapter 4.1.1. The still water bending moment is used in the design of the midship section using AH70 steel. The same still water bending moment is also used in fatigue assessment.

3.3.2 Vertical wave bending moment

Vertical wave bending moment is calculated according to the UR-S11A which is incorporated into the LR Rules for Ships Part 4, Ch. 8, Sec. 16. The vertical wave bending moment is calculated for both the hogging and sagging conditions. The equation used to determine moments on both conditions is obtained from the UR-S11A. The vertical wave bending moments are described in equation 10 (UR-S11A 2015, p. 9):

$$M_W = \pm 1.5 f_R L^3 C C_w \left(\frac{B}{L}\right)^{0.8} f_{NL-Hog} \quad (10)$$

where:

f_0 = Fraction of ships lifetime spent in transit, taken as:

$$f_R = 0.85$$

f_{NL} = Hogging or sagging correction factor, taken as:

Hogging:

$$f_{NL-Hog} = \min\left(0.3 \frac{C_b}{C_w} \sqrt{T}, 1, 1\right)$$

Sagging:

$$f_{NL-Sag} = \max\left(4.5 \frac{1+0.2f_{bow}}{C_w \sqrt{C_b L^{0.3}}}, 1\right)$$

f_{bow} = Bow flare shape coefficient, taken as:

$$f_{bow} = \frac{A_{DK} - A_{WL}}{0.2Lz_f}$$

A_{DK} = Projected area of the uppermost deck in m², approximate value is used based on existing ships

A_{WL} = Area at waterline in m² 0.8L fore of the aft perpendicular, approximate value is used based on existing ships

z_f = Vertical distance between the uppermost deck and the waterline at forward perpendicular

The vertical wave bending moment is calculated for strength assessment using the equation 10. For fatigue assessment the vertical wave bending moment is calculated using the CSR wave bending moment. Calculations for fatigue assessment are described in Section 3.7.

3.3.3 Hull girder stress

The hull girder stresses due to the still water and wave vertical bending moment are determined according to the UR-S11A. The permissible stress is calculated using partial safety factors to combine the effects of still water and vertical wave bending moments. The combined design stress is derived in equation 16 (UR-S11A 2015, p. 14):

$$\sigma_{HOG} = \frac{\gamma_s M_s + \gamma_w M_w}{I_{net}} (Z - Z_n) \cdot 10^{-3} \quad (16)$$

where:

γ_s = Partial safety factor, taken as:

$$\gamma_s = 1$$

γ_w = Partial safety factor, taken as:

$$\gamma_w = 1$$

Z = Vertical distance from the baseline of the location under consideration in m

Z_n = Vertical distance from the baseline to the neutral axis in m

This formulation of hull girder stresses due to vertical bending moments is done using LR software RulesCalc. RulesCalc software uses the formulation above to check a modelled midship section to fulfil the rule requirements. The use of RulesCalc is described in detail in Section 3.4 of this study.

3.4 Scantling design using RulesCalc

The scantlings are determined using LR RulesCalc software. RulesCalc is a software used to check designs for compliance with the Rules for Ships. RulesCalc checks the design automatically based on the selected set of rules. RulesCalc is used to check the scantlings for midship sections against longitudinal loads.

Midship section is modelled in RulesCalc. Modelling includes inputting the main dimensions of the ship as well as local scantlings of each structural member. The locations of transverse structures are also assigned in RulesCalc even as the study focuses on longitudinal structure. This is done as input if transverse structure is required by the RulesCalc software.

The RulesCalc is used to determine the minimum scantlings that will satisfy the rule requirements for local scantlings. RulesCalc determines local plate thicknesses based on the Rules for Ships Part 3 and Part 4. As local loads are not considered in this study, no further actions are made to determine local stresses.

RulesCalc follows the calculations described in Section 3.3. The midship section and initial data presented in Section 3.1 are used in RulesCalc. The modeled midship section is shown in Figure 8. The ballast tank arrangement of both midship sections is the same and can be seen from the Figure 8 marked with blue horizontal stripes.

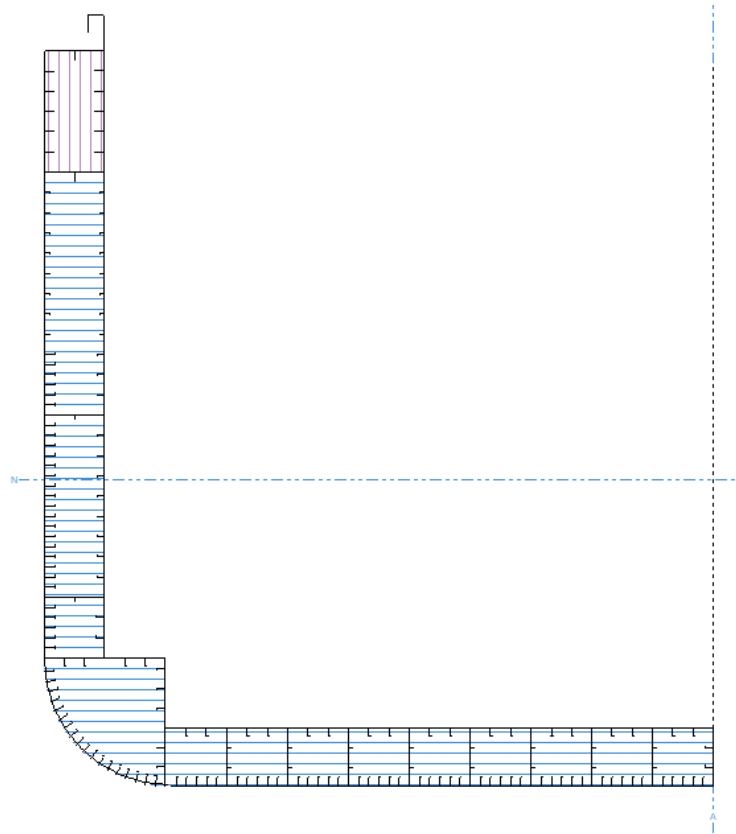


Figure 8. RulesCalc model of the midship section

The scantlings for both midship sections are determined by checking required values for every structural member. The scantlings are set to the limit values to minimize material use. After satisfying the local requirements of the rules, the hull girder section modulus values at hatch coaming, at main deck and at bottom are checked. Scantlings in both locations are increased so that the requirements are fulfilled.

Finally, moment of inertia is checked for UR S11A requirement as described in equation 8 in Section 3.3. This requirement is incorporated into the Rules for Ships Part. 4, Ch. 8, Sec. 16. As the study focuses on longitudinal strength, the UR-S11A requirements are driving the design. Although in the fatigue assessment only vertical bending moments are considered, other loads described in Section 3.3 are used for longitudinal strength assessment in RulesCalc to produce a realistic design.

3.5 High strength steel scantling design

As the high strength steel with yield strength of 690 MPa is not yet acknowledged by the Rules for Ships or by IACS, the RulesCalc software cannot calculate required scantlings when using steel with such a high yield strength. Scantling determination is done based on the design stress and allowable stress calculations provided by UR-S11A and presented in equations 9 and 16.

Containerships are considered as hogging vessels (Hong 2019). According to the consideration, the hull shape of containerships and the cargo- and lightship weight distribution over the ship's length causes the ship to be always in hogging condition. For this reason, the highest allowable stress is calculated only for hogging condition where the highest combined bending moment occurs. The bending stress is calculated according to equation 16 described in Subsection 3.3.3.

The design stress is calculated for highest longitudinally effective member, in this case the top plate of hatch coaming. The design stress, or hogging stress, is not to exceed the allowable stress in the top plate of the hatch coaming. The allowable stress is calculated according to UR-S11A (2015, p. 15) as described in equation 9 in Section 3.3.

As the local scantlings are excluded from the study, the effects of local scantling limits are not calculated for the midship section with high strength steel. The minimum plate thicknesses are taken from RulesCalc model for normal grade steel in order to have same requirements for both midship sections and to produce a realistic design.

The used material values for high strength steel AH70 are the same as in AH47 steel with yield strength of 460 MPa, except the yield strength, ultimate strength, and the k_L factor. Value for the k_L factor is selected based on Section 2.4. The values of the used AH70 steel are shown in Table 6 with other steels used in the design.

Table 6. Mechanical properties of used steels

Steel	AH32	AH36	AH40	AH47	AH70
Yield strength R_{eh}	315 MPa	355 MPa	390 MPa	460 MPa	690 MPa
Design ultimate strength R_m	440 MPa	490 MPa	510 MPa	570 MPa	840 MPa
k_L factor	0.78	0.72	0.68	0.62	0.53

Milder steels than AH47 are used in the midship sections where it is not beneficial to use higher strength steels. Typically, the steels with lower yield strength are used in structural members close to the neutral axis of the midship section. Steel grades EH and DH are also used in the midship section where required by the Rules for Ships (Lloyd's Register 2019, pp. 179-181). These steels have the same mechanical properties as AH steels based on the number in steel name, i.e. EH47 is assumed to have same mechanical properties as AH47.

Initial midship section with AH47 steel has a 2.36% margin in the maximum bending stress at hatch coaming. The same margin acts as a limit when designing the midship section using high strength steel AH70. The scantlings are reduced at maximum to the point where the bending stress is 2.36% over the permissible stress to have the same amount of margin in stress as the initial midship section with AH47 steel. This is done to ensure comparability of the two midship sections.

Hull cross section moment of inertia and local scantling limits are followed and the midship section is designed to those limits. If one of the limits prevents the reducing of scantlings to the point that the bending stress is 2.36% of the permissible stress, the scantlings are designed to the limit value even if the margin is bigger than 2.36%. Bending and permissible stress calculations are presented for initial midship section with AH47 steel and for midship section designed using high strength steel AH70 in Subsection 4.2.1.

3.6 Locations for fatigue assessment

Locations for fatigue life calculations were selected based on Section 2.4. The reference fatigue calculation is made considering only vertical bending moments as is done in 4R fatigue calculations due to the limits of 4R method. As the considered fatigue loading is only the vertical global bending moment, the highest stresses can be assumed to happen in the locations furthest from the neutral axis.

Container ships are considered as hogging type of ships (Hong 2019). For this reason, the maximum stresses are assumed to occur in the hogging condition. Because of this the highest tensile stress ranges occur in locations above the neutral axis of the cross section, all the locations are selected from the upper part of midship section.

Critical locations are selected to be on the longitudinal end connections of a non-watertight bulkhead. The selected critical locations have geometry that can be found in various kind of ship types as well as in container ships. Two joints common to various ship types are selected, and a container ship specific location at top torsion box. The three selected locations are used in fatigue calculations. These locations are numbered as 1, 2 and 3. The locations are marked in Figure 9.

WEB SECTION

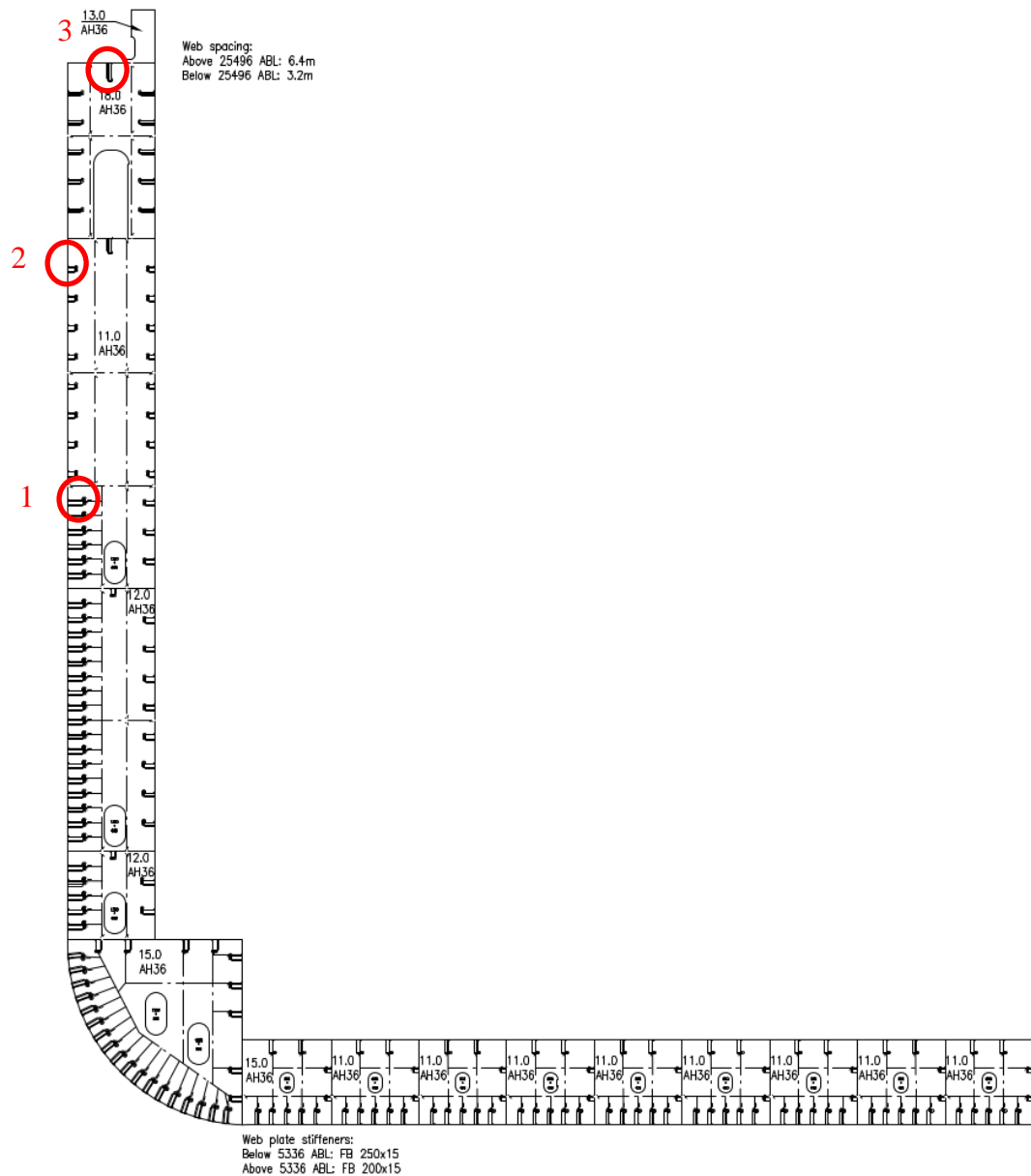


Figure 9. Critical fatigue locations

Selected location 1 represents an ice strengthening structure. Similar type of structural detail could be used in other ice going ship types. The location 1 is selected as the ice strengthened structure furthest away from the neutral axis on the tensile side of cross section.

Location 2 is selected as it is a typical longitudinal end connection found in numerous types of ships. The selected location is chosen as it is furthest away from the neutral axis while having a common geometry. Location 3 is a typical stiffener structure found in container ships. The thick stiffener attached to a thick main deck without bracket at the end connection is used in container ship top torsion box to provide moment of inertia and stiffness to the cross section.

These locations are checked using the 4R fatigue assessments. Rule based fatigue life calculation based on the CSR is made for location 3 as well as 4R fatigue life calculation. The drawings of non-watertight bulkhead and midship section are used as a base for modelling 3D FEA for 4R calculations.

3.7 Rule based fatigue life

Fatigue life of critical details is determined using the CSR fatigue damage calculation to provide a reference point for 4R method. The fatigue damage calculation presented in the CSR is based on a Palmgren-Miner damage sum for a given design life. The damage sum represents the amount of fatigue damage produced to the location under consideration. (IACS 2019a, pp. 551-553.)

Fatigue life of a ship is usually described in years instead of number of cycles. This makes sense as ships encounter enormous number of waves during their lifetime. Fatigue life is determined using a design life of 20 years. The CSR gives service time factor values for bulk carriers and tankers but not for containerships. In this study the ship is assumed to be in service during 85% of its lifetime. The ship is assumed to be in one loading condition for better comparison as stated in Subsection 1.5.1.

Elementary fatigue life for each loading condition is calculated in the CSR. The elementary fatigue damages are then added together to form a total fatigue damage. As the ship is assumed to be in one loading condition in this study, the elementary fatigue life for one loading condition is taken as the total fatigue damage. The fatigue damage is calculated according to equation 17 (IACS 2019, p. 552).

$$D_e = \frac{a \cdot N_D}{K_2} \frac{\Delta \sigma_{FS}^m}{\ln(N_r)^{\frac{m}{\zeta}}} \cdot \mu \cdot \Gamma \left(1 + \frac{m}{\zeta} \right) \quad (17)$$

where:

N_D = Number of wave cycles during the design fatigue lifetime, taken as

$$N_D = 31.557 \cdot 10^6 \frac{f_0 T_D}{4 \log(L)}$$

f_0 = Service factor, taken as

$$f_0 = 0.85$$

T_D = Design lifetime in years, taken as

$$T_D = 20$$

a = Fraction in each loading condition, taken as

$$a = 1$$

$\Delta \sigma_{FS}$ = Fatigue stress range in N/mm² with reference probability of exceedance of 10⁻²

N_r = Corresponding number of cycles to probability of exceedance of 10⁻², taken as

$$N_r = 100$$

ζ = Weibull shape parameter, taken as

$$\zeta = 1$$

$\Gamma(x)$ = Complete gamma function

μ = Coefficient for change of inverse slope of S-N curve, taken as

$$\mu = 1 - \frac{\left\{ \gamma \left(1 + \frac{m}{\zeta}, v \right) - v^{-\frac{\Delta m}{\zeta}} \cdot \gamma \left(1 + \left(\frac{m + \Delta m}{\zeta} \right), v \right) \right\}}{\Gamma \left(1 + \frac{m}{\zeta} \right)}, \text{ in air environment}$$

$\mu = 1$, corrosive environment

$$v = \left(\frac{\Delta \sigma_q}{\Delta \sigma_{FS}} \right)^{\zeta} \ln(N_r)$$

$\gamma(x, y)$ = Incomplete gamma function

$\Delta \sigma_q$ = Stress range at intersection of S-N curve segments, taken as

$$\Delta \sigma_q = 100.2 \text{ N/mm}^2$$

Δm = Change in inverse S-N curve slope at 10⁷ cycles, taken as

$$\Delta m = 2$$

$K1, K2$ = S-N Curve coefficients, taken as

$$K1 = 3.988 \cdot 10^{12}$$

$$K2 = 1.52 \cdot 10^{12}$$

Using the calculated fatigue damage according to equation 17, fatigue life in years can be calculated. The fatigue life is calculated according to CSR fatigue life calculation. Equation 18 presents the calculation of fatigue life T_F .

$$T_F = \frac{T_D}{D_e} \quad (18)$$

The hot spot stress range are calculated according to simplified stress analysis described in the CSR. The simplified stress analysis uses nominal stress and tabulated stress concentration factors to determine hot spot stress range. The rule-based fatigue life is calculated for location 3 with a stress concentration factor of 1.36 (IACS 2019a, p. 571).

Stress due to wave bending moment is calculated according to the CSR instead of UR-S11A. UR-S11A is used for longitudinal strength assessments. Wave bending moment in the CSR is calculated according to equation 19 (IACS 2019a, p. 187).

$$M_{wv-f} = 0.19 f_{NL} f_m f_p C_w L^2 B C_B \quad (19)$$

where:

f_{NL} = Non-linear coefficient, taken as

$$f_{NL} = 1$$

f_m = Distribution factor along the length of the ship, taken as

$$f_m = 1$$

$$f_p = 0.9(0.27 - (6 + 4f_t)L) \cdot 10^{-5}$$

f_t = Ratio between scantling draught and draught at loading condition

$$f_t = 1$$

In the fatigue assessment the still water bending moment is assumed to be maximum still water bending moment in hogging condition. Hull girder stress is calculated for maximum and minimum wave bending moment to obtain hull girder stress range. Hull girder stress for fatigue assessment in N/mm^2 is calculated according to equation 20.

$$\sigma_{HS} = f_c K_a \left(\frac{M_{wv-f}}{I} \right) (z-z_n) \cdot 10^{-3} \quad (20)$$

where:

$f_c = 0.95$ (IACS 2019a, p. 525)

K_a = stress concentration factor, taken as

$K_a = 1.36$ (IACS 2019a, p. 571, table 4)

Hull girder stress range is used to calculate fatigue stress range $\Delta\sigma_{FS}$. Fatigue stress range is calculated according to CSR. Calculation is made according to equation 21 (IACS 2019a, p. 542).

$$\Delta\sigma_{FS} = f_{mean} f_{thick} f_{warp} \Delta\sigma_{HS} \quad (21)$$

where:

f_{mean} = coefficient for mean stress effect, taken as

$$f_{mean} = \min \left[1, 0.9 + 0.2 \left(\frac{\sigma_{mean}}{2\Delta\sigma_{HS}} \right) \right]$$

$$\sigma_{mean} = f_c K_a \left(\frac{M_s}{I} \right) (z-z_n) \cdot 10^{-3}$$

f_{thick} = coefficient for thickness effect, taken as

$$f_{thick} = \left(\frac{t}{22} \right)^{0.1}$$

t = Plate thickness in mm

f_{warp} = coefficient for warping stress, taken as

$f_{warp} = 1$, as warping is not considered

Rule-based fatigue life is determined for one of the selected locations. Location is selected based on selection presented in Section 3.6. Result of the rule-based fatigue calculations are presented in Section 4.3.

3.8 4R method

4R method for fatigue assessment is a method described by Björk et. al. (2018) for a fatigue strength assessment of a duplex and super-duplex stainless steel. The method is created to include the effect of material strength, local geometry of the joint, mean stress and residual stresses into fatigue life calculation. The method is based on the effective notch stress

method (ENS). Four Rs in the name stand for: ultimate strength of material R_m , local joint geometry R_{true} , applied stress ratio R and residual stresses σ_{res} . 4R method utilizes conversion of available global stress range to local elastic-plastic behavior at the joint. By utilizing the conversion, the 4R method estimates the fatigue strength of the joint based on this local elastic-plastic behavior by means of R_{local} . (Björk et al. 2018, pp.1-2.)

4R method calculates the cycles to failure of a welded joint. To be able to calculate the cycles, input values for ultimate strength of material, joint geometry, applied stress ratio and residual stresses are needed to be considered. The cycles to fatigue failure are calculated according to equation 22 (Ahola, Skriko & Björk 2019, p. 10).

$$N_{f,4R} = \left(\frac{\sqrt{1-R_{local}}}{\Delta\sigma_k} \right)^{m_{4R}} C_{4R} \quad (22)$$

where:

R_{local} = Local stress ratio

m_{4R} = S-N curve slope of 4R, taken as

$m_{4R} = 5.85$

C_{4R} = Characteristic fatigue capacity with probability of 97.7%, taken as

$C_{4R} = 10^{20.83}$

$\Delta\sigma_k$ = Effective notch stress range in N/mm²

ENS range $\Delta\sigma_k$ considers the nominal stress in the joint as well as the effect of joint geometry and notch effect of the weld. The nominal stress is caused by global bending moments, still water and wave bending moment. calculating the nominal stress at the location away from the joint geometry caused by the global bending moments. The ENS stress range is calculated according to equation 23.

$$\Delta\sigma_k = K_{s,m} K_{t,m} \Delta\sigma_{HOG} + (K_{s,b} - 1) K_{t,b} \Delta\sigma_{HOG} \quad (23)$$

Structural stress caused by the joint geometry is calculated by multiplying the nominal stress by structural stress concentration factors K_s . These factors are calculated as $K_{s,m}$ membrane loading and $K_{s,b}$ bending loading separately. The structural stress is then multiplied by notch stress concentration factors K_t caused by the notch effect of the weld. Like structural stress

concentration factors, factor $K_{t,m}$ for membrane and $K_{t,b}$ for bending loading are calculated separately.

Stress concentration factors $K_{s,m}$, $K_{s,b}$, $K_{t,m}$ and $K_{t,b}$ are defined for membrane and bending stress separately using a 3D finite element analysis. The model is constructed according to the IIW recommendations for ENS finite element models (Hobbacher 2014, p. 30). The actual joint geometry is modelled to take the structural stress concentration into account. The weld geometry is also modelled in detail with an assumed notch radius of 1 mm. By modelling the weld, the notch effect can be considered as well. By modelling the joint in detail, the combined effect $K_s \cdot K_t$ can be read from the finite element analysis.

As the thickness of the longitudinal members is small compared to the height of the ship, the bending stress gradient over the thickness of a longitudinal stiffener is small. Because of this the stress gradient over the thickness of the longitudinal stiffener is neglected. Ahola and Björk (2020) are conducting a study on stress concentrations. The stress distribution they found is suitable for this case as well. The distribution of stresses is shown in Figure 10.

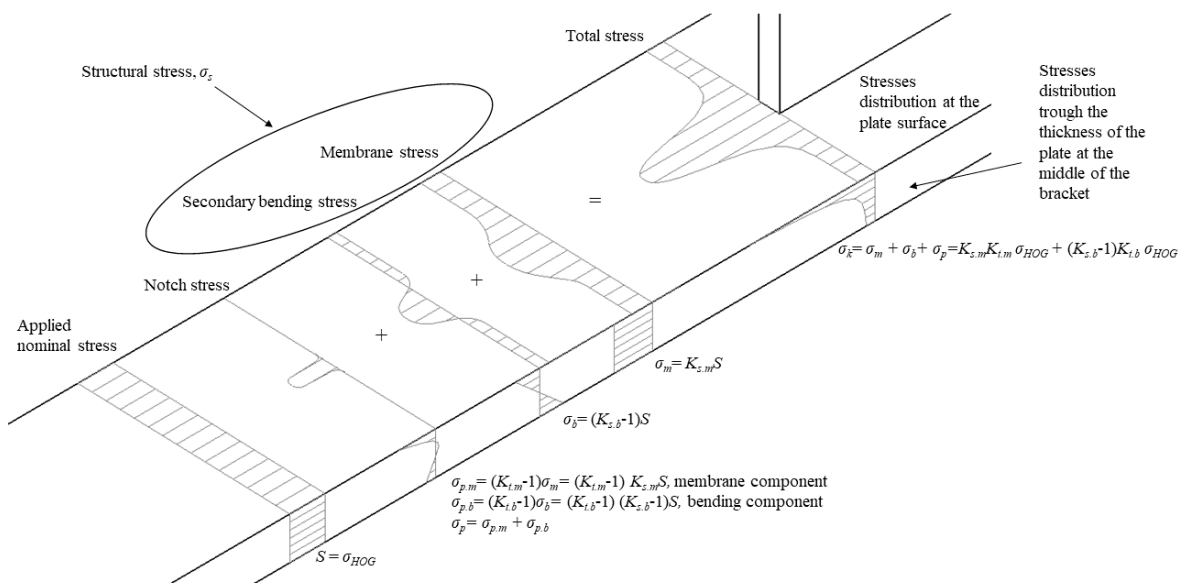


Figure 10. Stress distributions (Ahola & Björk 2020).

In the Figure 10, the total stress at weld is shown as a distribution over the width and over the thickness of a longitudinal stiffener flange when the loading S is membrane loading. ENS

stress σ_k consists of nominal membrane stress σ_m , secondary bending stress σ_b and non-linear notch stress σ_p . As the structural and notch stresses are dependent on the nominal stress by stress concentration factors, the ENS stress at the weld toe is calculated as shown in equation 23.

Local elastic-plastic behavior R_{local} at the notch of the joint is calculated based on Ramberg-Osgood material model. The Ramberg-Osgood material model is presented in equation 24. The strain of the material can be calculated according to Neuber's rule presented in equation 25. (Björk et al. 2018, p. 3.)

$$\Delta\varepsilon = \frac{\Delta\sigma}{E} + \left(\frac{\Delta\sigma}{H}\right)^{\frac{1}{n}} \quad (24)$$

$$\Delta\varepsilon = \frac{(\sigma_k + \sigma_{res})^2}{\sigma E} \quad (25)$$

where:

H = Strength coefficient

$$H = 1.65R_m$$

n = Strain hardening component

$$n = 0.15$$

$\sigma_{k,max}$ = Maximum applied ENS stress

Residual stress σ_{res} is assumed as the welding method is not known. Gannon et al. (2012, p. 33) and Kenno et al. (2010, pp. 272-273) found out that high residual stresses in welds between plating and stiffener sometimes exceeding the yield strength of the stiffener material. Based on these findings the residual stress in welds connecting longitudinal stiffeners to web plate stiffeners or brackets are assumed to have a value of yield strength of the material of surrounding structure.

By setting the equations 24 and 25 to be equal the maximum local stress can be calculated. Close form solution cannot be found on the equation, so numerical solving is used.

Numerical solving is done using Microsoft Excel's GRG Nonlinear numerical solver. Maximum stress at notch σ_{max} is solved from equation 26.

$$\frac{\sigma_{max}}{E} + \left(\frac{\sigma_{max}}{H}\right)^{\frac{1}{n}} = \frac{(\sigma_{k,max} + \sigma_{res})^2}{\sigma_{max}E} \quad (26)$$

Local minimum stress happens at the lower point of stress hysteresis loop. Masing equation that is presented in equation 27 and Neuber's rule are used to calculate local stress range. (Björk et al. 2018 pp, 3-4.) The local stress range can be calculated by setting the Masing equation and Neuber's rule to be equal. Equation 28 is used to calculate local stress range.

$$\Delta\varepsilon = \frac{\Delta\sigma}{E} + 2\left(\frac{\Delta\sigma}{2H}\right)^{\frac{1}{n}} \quad (27)$$

$$\frac{\Delta\sigma}{E} + 2\left(\frac{\Delta\sigma}{2H}\right)^{\frac{1}{n}} = \frac{(\Delta\sigma_k)^2}{\Delta\sigma E} \quad (28)$$

After solving the local stress range at the notch, the local stress ratio can be calculated. The local stress ratio R_{local} can be calculated. R_{local} is needed as an input to the main equation of 4R method presented in equation 22. Local stress ratio is calculated using equation 29 (Björk et al. 2018, p. 3).

$$R_{local} = 1 - \frac{\Delta\sigma}{\sigma_{max}} \quad (29)$$

If fatigue life reduces when moving from commonly used steels to high strength steel, post weld treatments can be included in the fatigue assessment by addressing lower residual stress values. High frequency mechanical impact (HFMI) treatment is used in the calculations if it is necessary to achieve sufficient fatigue life. Residual stress then taken as $\sigma_{res} = -0.255R_m$ (Björk et al. 2018, p.5).

HFMI treatment is a post weld treatment method where the weld toe is peened with a HFMI equipment. In the HFMI treatment the weld toe region is peened with a cylindrical tool head at a 90 Hz frequency. HFMI term includes multiple different kinds of peening methods

including ultrasonic peening and pneumatic peening. With the use of HFMI treatment compressive residual stresses can be introduced into the structure. The FAT class of a joint can increase significantly after applying the HFMI treatment. (Marquis & Barsoum 2016, pp. 5, 17-21.)

As the HFMI treatment causes compressive residual stresses, there may be a case where local stress range is below the stress range limit value for fatigue to happen. Fatigue stress range limit is calculated according to equation 30 for case of compressive residual stresses.

$$\Delta\sigma_{k,limit} = \sigma_{res}(1-R) \quad (30)$$

where:

σ_{res} = Absolute value of residual stress

R = Applied stress ratio

If the ENS stress range $\Delta\sigma_k$ is below the limit stress range value, it is assumed that no fatigue happens in the joint. The stress range limit value is calculated for each location. The values of limit stress range and applied stress ranges are shown in 4.5.

3.8.1 Stress concentration factors for 4R calculations

FEA is used to obtain local stress concentration factors for 4R fatigue life calculation. FEA is done using ABAQUS CAE software published by Dassault Systems/SIMULIA. All the analyses are calculated using linear models and ABAQUS/Standard integrated solver. The used version of ABAQUS CAE is 2019.HF4.

The critical locations for fatigue life calculations are modelled on detail. The locations modelled are selected locations in Section 3.6. The connections of the critical locations are modelled in detail and meshed with a very dense mesh.

4R method uses same structural stress and notch stress concentration factors as ENS. The ENS method described by Hobbacher (2014, pp. 29-30) gives guidance of how to create a FEA model to be used in determining the stress concentration factors. Model and mesh of location 3 is presented in Figure 11.

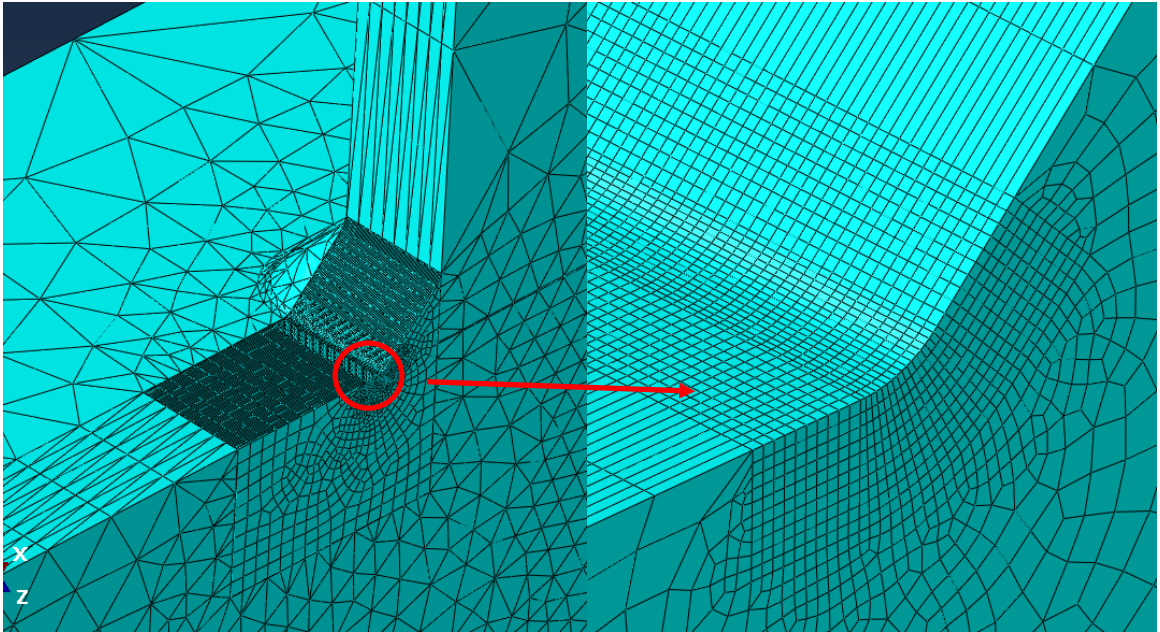


Figure 11. Dense mesh of location 3

Weld toe is meshed using a separate part which is meshed with 8-node solid hexahedral elements with an element size of 0.1 mm. The weld toe area is connected to the surrounding structure by using tie constraints. The tie constraint connects surfaces of the weld toe region to surrounding structure. The use of tie constraints allows different meshing techniques in the surrounding structure than in the weld toe region. Surrounding structure is meshed with tetrahedral solid elements to reduce modelling time. The surrounding tetrahedral mesh is not expected to affect the results of the tightly meshed weld toe area, the purpose of the surrounding mesh is to produce proper stresses and strains to the boundary of densely meshed weld toe area.

Model is loaded separately with membrane and bending load. Separate stress concentration factors are needed for 4R calculation. Deriving the two load cases are described in Section 3.8. Model is loaded with a 1 MPa membrane loading so the stress concentration factor $K_{s,m} \cdot K_{t,m}$ can be read directly from the weld toe. 1 MPa membrane loading is acquired by loading the model by applying a pressure with value of -1 MPa to the end of the model. The loading of location 3 is shown in Figure 12.

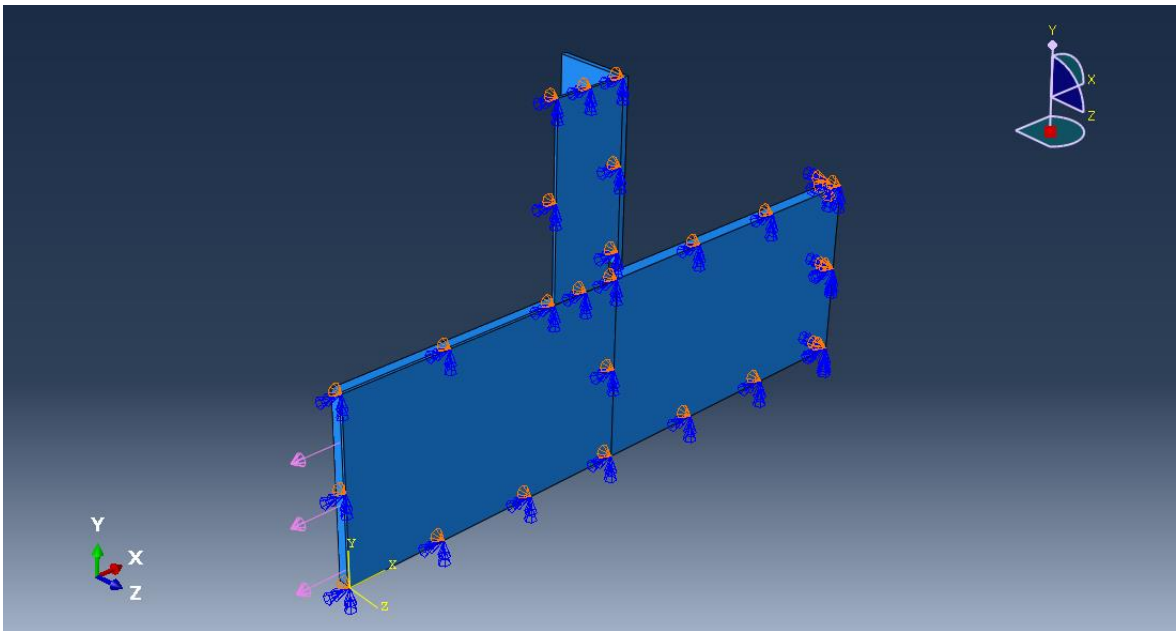


Figure 12. Membrane loading

Stress concentration for bending $K_{s,b} \cdot K_{t,b}$ is acquired using the same model as in membrane loading. In bending analysis, the model is loaded with a pressure varying linearly from -0.5 MPa to 0.5 MPa over the height of a stiffener to the end of the model. The loading of location 3 with bending loading is shown in Figure 13.

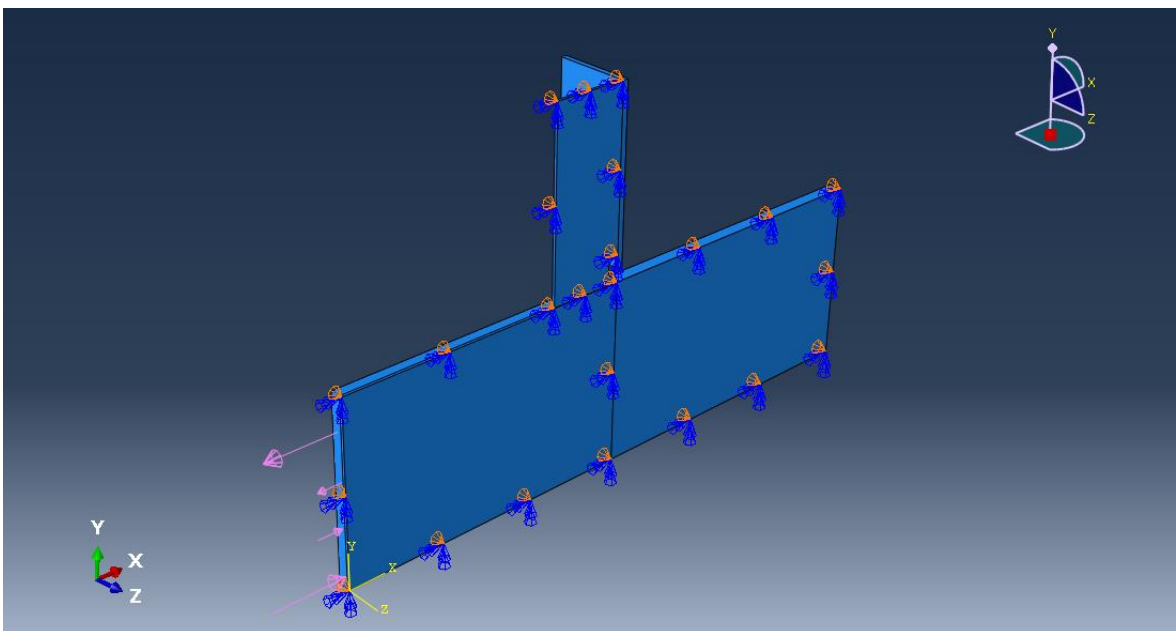


Figure 13. Bending loading

Boundary conditions of the model can also be seen on the Figure 12 and Figure 13. Opposite end of the model compared to the loaded end is constrained using fixed boundary conditions. In locations where the web of a longitudinal stiffener is arranged vertically and where the joint is symmetrical, half of the joint is modelled. A symmetry constraint is applied to the surface on the symmetry line. For locations where the web of a longitudinal stiffener is arranged vertically, the entire connection is modelled.

3.9 Unit weight calculation

Unit weight of both midship sections are calculated. The unit weight is calculated for one meter of parallel midship section. The unit weight of the midship section can be obtained from RulesCalc, as shown in Figure 14. The software calculates weight as kg/m for parallel midship section.

53	Centroid Y	m	0.000
54	Centroid Z	m	13.010
55	Inertia YY'	m ⁴	1,376.970
56	Inertia ZZ'	m ⁴	5,568.813
57	Principal Axis Angle	deg	0.000
58	Weight/Unit length	kg/m	79,927.034

Figure 14. Weight/Unit length obtained from RulesCalc of midship section using AH47.

RulesCalc assumes the density of steel to be 7850 kg/m³. This assumption is made for all steels with different strengths used in the calculations. The assumed weight loss $W\%$ is calculated according to equation 31.

$$W\% = 100\% \cdot \frac{W_{AH47} - W_{AH70}}{W_{AH47}} \quad (31)$$

where:

W_{AH47} = Unit weight of midship section made using AH47 steel in kg/m

W_{AH70} = Unit weight of midship section made using AH70 steel in kg/m

The obtained weight values are presented in Section 4.7. Also, the calculated weight difference is presented along with the obtained weight results. The unit weight results are discussed in Chapter 5.

4 RESULTS

Results of the study are presented in this chapter. The results are obtained based on the methods described in Chapter 3. Key results and key findings are analyzed in Chapter 5. The results and findings are also discussed in the Chapter 5.

4.1 Global loads acting on the ship with AH47 midship section

Global loads acting on the ship are extracted from RulesCalc. As mentioned in Section 3.3 the loading of the ship is calculated using RulesCalc software. The software calculates the loads based on the UR-S11A which are presented in Section 3.3.

4.1.1 Still water and wave bending moments

The still water bending moment was determined as described in Subsection 3.3.1. Still water bending moment was determined for the midship section only as that is the location studied. Calculated still water bending moment is presented as a bending moment distribution along the length of the ship in Figure 15. In the same figure, the vertical wave bending moments are presented as a distribution along the length of the ship. The maximum value is calculated as described in Subsection 3.3.2.

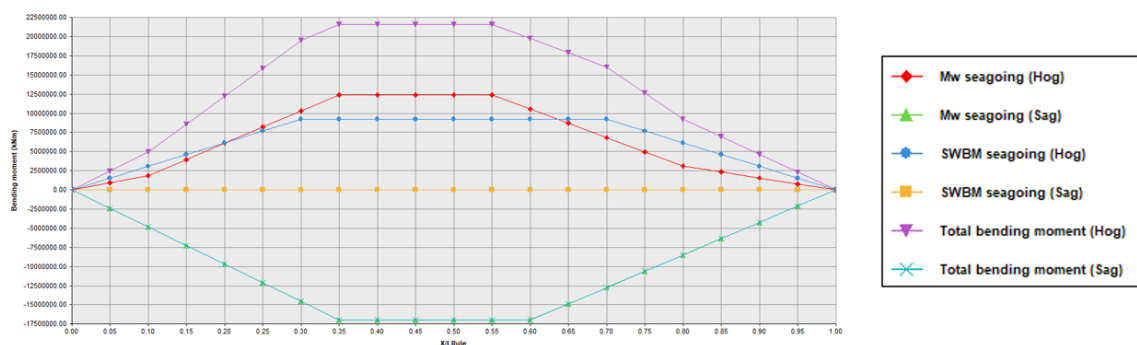


Figure 15. Bending moments

The values used in the study are obtained for the location $x = 0.5L$, as the midship section is located at the half length of the ship. In the Figure 15, still water bending moment is marked with blue line, wave bending moment is marked with red line, and a sum of these named

total bending moment is marked with a purple line. The still water and wave bending moments for the location $x = 0.5L$ are presented in Table 7.

Table 7. Still water and wave bending moments at location $x = 0.5L$

Max SWBM Hog	kNm	9 200 000
Max SWBM Sag	kNm	0
Wave bending moment (hogging)	kNm	12 402 795
Wave bending moment (sagging)	kNm	-16 992 801

The wave bending moments are related to ship's main dimensions as described in Subsections 3.3.2. Consequently, as the hull form does not affect the rule wave bending moment directly the calculated wave bending moments are realistic even the hull form is not known. Still water bending moment is derived from data of existing ships to get a realistic value.

4.2 Midship section designed using AH70 steel

The ordinary midship section designed using AH70 high strength steel is presented in Figure 16. Longitudinal structures are designed using high strength as described in Section 3.5. Transverse bulkhead structure presented in appendix IV is not altered as the study focuses on longitudinal structures. Only the length of stiffening in the double bottom web plating is altered according to bottom longitudinals.

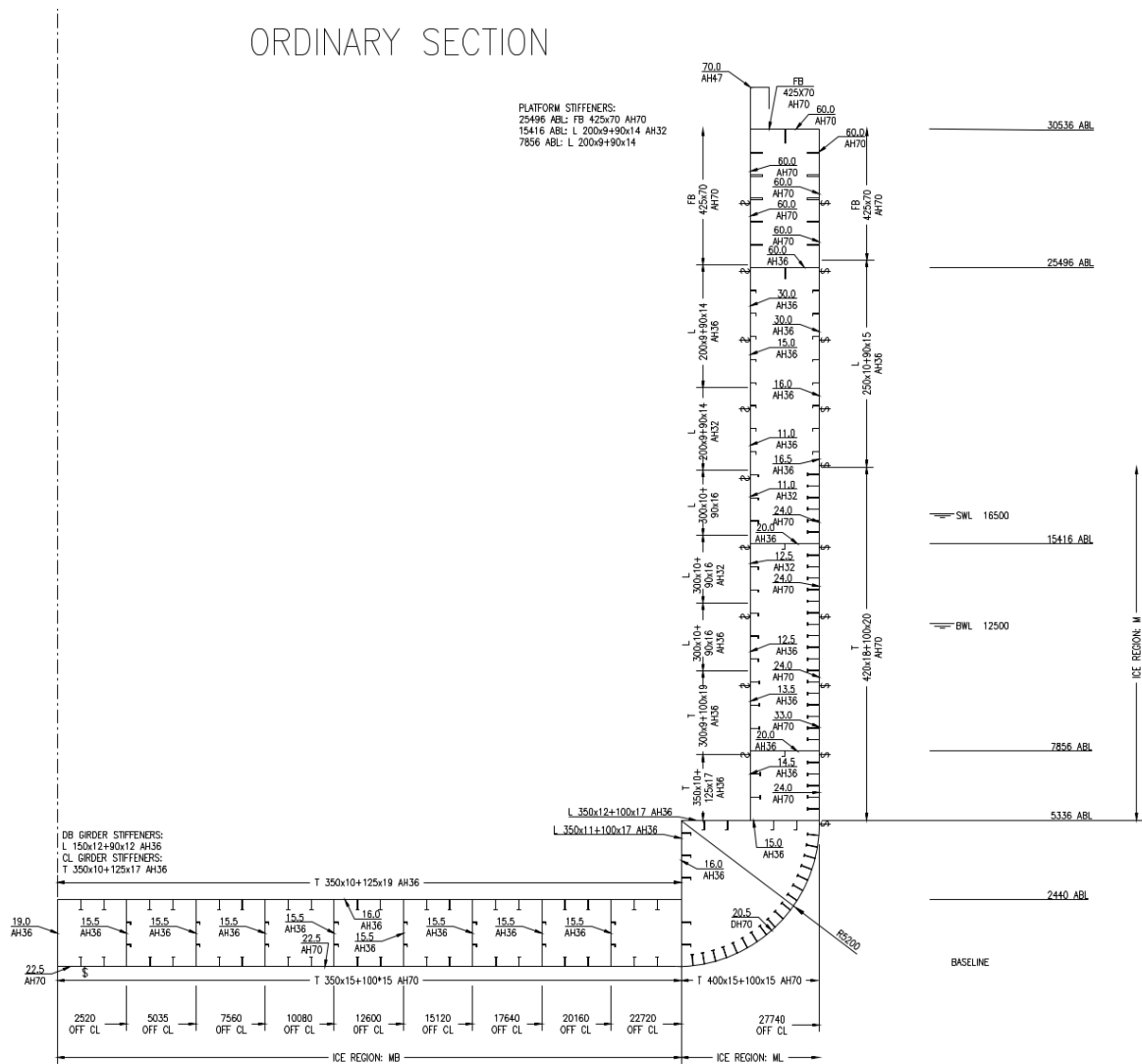


Figure 16. Ordinary midship section designed using high strength steel

Midship section presented in Figure 16 is designed to ice class PC-3. The ice strengthening structure is designed from AH70 high strength steel as well. In addition to ice strengthened structure, hatch coaming and main deck structures designed using AH70 steel. Complete drawing of the midship including web section can be found in the appendix III.

4.2.1 Hull girder stress according UR-S11A

Bending stress and limit moment of inertia is calculated according to UR-S11A as described in Subsection 3.3.3. The bending stress calculations include required moment of inertia. Calculations for initial midship section are presented in Table 8.

Table 8. UR-S11A results

Results of UR-S11A hull girder stress calculations		
Ship	Inertia above limit	Stress below limit
Initial midship section, AH47	8.79%	2.36%
Midship section with high strength steel, AH70	0.11%	14.03%

The calculations are presented for both midship sections for comparison. Stresses are presented in maximum loading condition where the still water bending moment is at its maximum. This condition is hogging condition as mentioned in Section 3.5. Complete calculations for hull girder stress according to UR-S11A can be found in appendix I.

4.3 Rule based fatigue life calculations

CSR rule-based fatigue life was determined for location 3. The fatigue life calculation is made according to the methodology described in Section 3.6. The result of the CSR fatigue life calculation is presented in Table 9.

Table 9. CSR rule-based fatigue life of location 3

Rule-based fatigue life calculation for location 3		
$D_e=$	0.88	CSR Elementary fatigue damage
$T_f=$	22.6	a CSR Fatigue life

The calculated rule-based fatigue life is shown as a comparison in 4.6. The rule-based fatigue life exceeds the design fatigue life limit of 20 years. The fatigue lives including rule-based fatigue life is analyzed and discussed in Chapter 5.

4.4 Stress concentration factors

Stress concentration factors were determined according to Subsection 3.8.1. The stress concentration factors were obtained from local FEA. Maximum principal stress of an element was used as an output data when reading stress concentration factors from the

models. FEA model with calculated result of membrane stress concentration factor is shown in Figure 17. Figures of all stress concentration factors for each location are presented in appendix V.

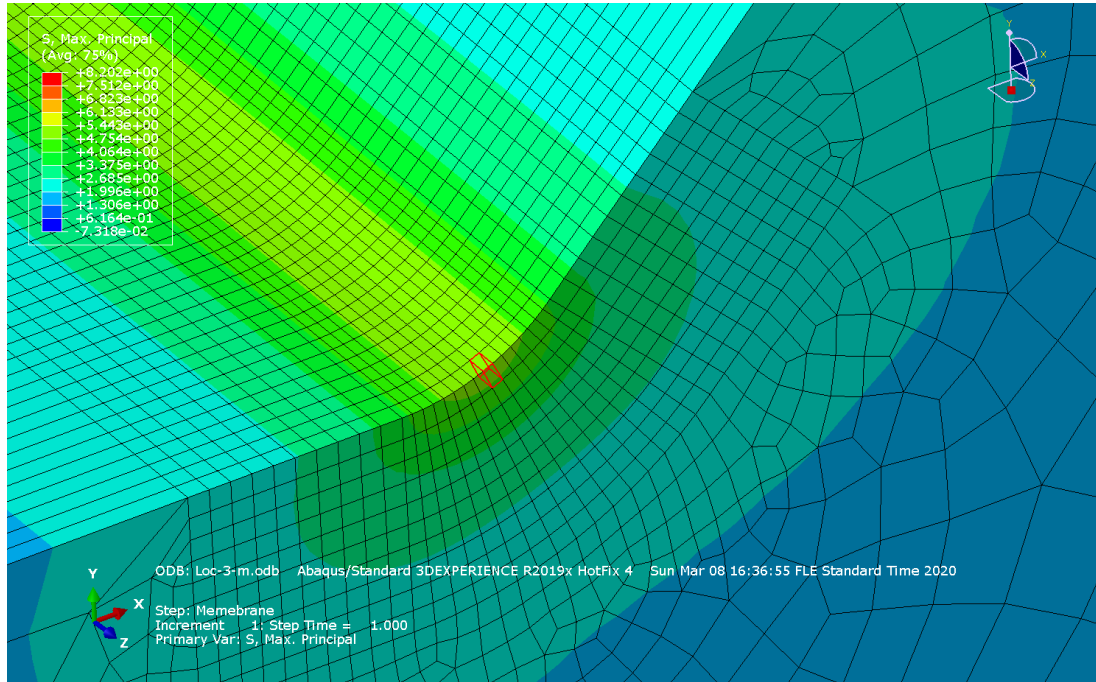


Figure 17. Membrane stress concentration factor for location 3

Stress concentration factors for ENS calculations were red from weld toe where either a web stiffener or a bracket joins to a longitudinal stiffener. Transverse structure where the end connection is located is a non-watertight bulkhead at midship section of the ship. Obtained stress concentration factors are presented in Table 10.

Table 10. Stress concentration factors

Stress concentration factors for 4R calculations						
Location $K_s \cdot K_t$	1		2		3	
	Membrane	Bending	Membrane	Bending	Membrane	Bending
AH47	5,02	0,02	4,66	4,18	5,09	5,68
AH70	4,92	0,05	4,66	4,18	5,09	5,68

The geometries of the locations are the same in locations 2 and 3 because the plate thicknesses and scantlings could not be reduced by using AH70 steel in construction. Location 1 is an ice strengthened location where the geometry of the joint changes when using AH47 or AH70 as construction material.

4.5 4R fatigue life calculations

For the 4R fatigue life calculations, the same reduced wave bending moment was used that was defined for rule-based fatigue life calculation. The 4R method also considered the effect of still water bending moment unlike the rule-based method in stress calculation. The still water bending moment and wave bending moment time distribution are shown in Figure 18.

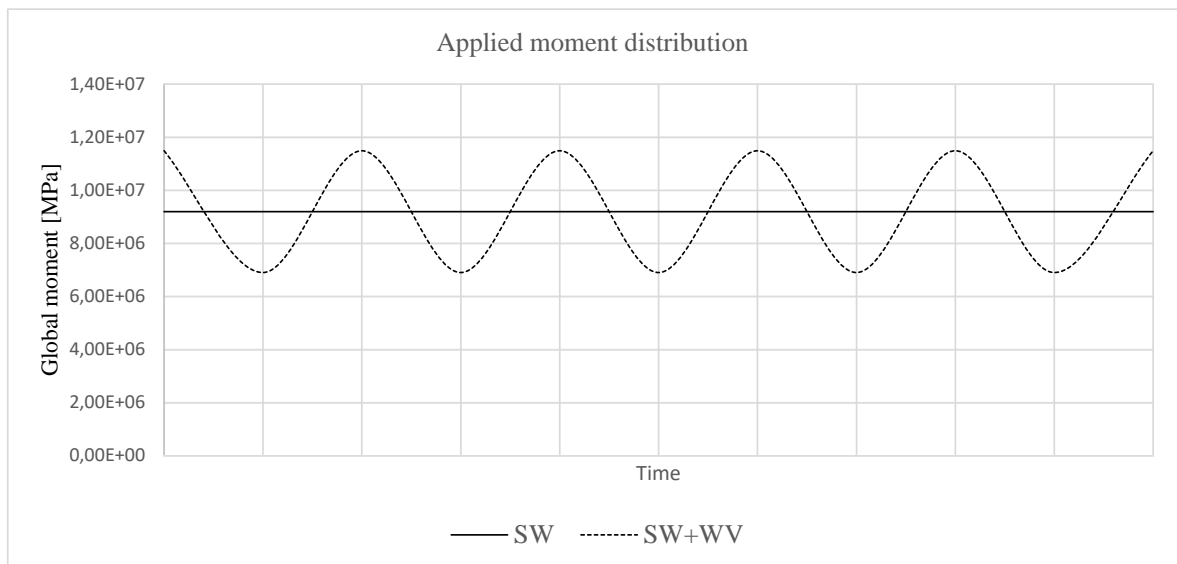


Figure 18. Still water and wave bending moment time distribution

The stress ranges for the 4R fatigue calculations are shown in Table 11. Values are shown for all the locations of midship sections with AH47 and AH70 steel. The stress amplitudes and the stress ratio R of applied load is presented. Also, the assumed residual stresses are shown for all cases including HFMI treated cases.

Table 11. 4R stress values

Stress values for 4R method				
	$\Delta\sigma_k$ [N/mm ²]	σ_{mean} [N/mm ²]	σ_{res} [N/mm ²]	R
AH47				
Location 1	83	33	460	0.60
Location 2	181	78	460	0.60
Location 3	294	115	460	0.60
AH70				
Location 1	77	31	690	0.60
Location 2	186	80	690	0.60
Location 3	308	121	690	0.60
AH70 HFMI				
Location 1	77	31	-214	0.60
Location 2	186	80	-214	0.60
Location 3	308	121	-214	0.60

Fatigue life using 4R method was calculated for all three locations according to Section 3.8. Fatigue life is calculated for both midship section using AH47 and AH70 steels. As stated in Section 1.6 the hypothesis is that the use of high strength steel AH70 leads to reduced fatigue life, fatigue life post weld treated connection was also calculated. Fatigue life values of both midship sections are presented in Table 12.

Table 12. 4R fatigue life calculation results

4R fatigue lives in cycles to failure and HFMI stress ranges					
	AH47	AH70	AH70 HFMI	$\Delta\sigma_k$ HFMI [N/mm ²]	$\Delta\sigma_{k,limit}$ [N/mm ²]
Location 1	30 312 000	16 014 000	-	77	86
Location 2	2 300 000	944 000	16 224 000	186	86
Location 3	502 000	175 000	571 000	308	87

The fatigue lives calculated using 4R method are described in cycles to failure. Location 1 fatigue life for AH70 HFMI case is not calculated as the ENS stress range is below the stress range limit for fatigue. No fatigue happens if the ENS stress range is below limit stress range

value. Characteristic fatigue life is calculated and probability of 97.7% is assumed as described in 3.8. 4R fatigue lives are compared between each other in Section 4.6.

4.6 Comparison of fatigue lives

The fatigue lives are compared to each other in Table 13. The percentual difference in 4R fatigue life between midship section using AH47 and midship section using AH70 is calculated and presented in the same table. Also, the fatigue life of HFMI treated connections are presented.

Table 13. Comparison of fatigue lives

Percentual difference between AH70 and AH47 fatigue lives			
	AH70/AH47	HFMI/AH47	
Location 1	53%	-	
Location 2	41%	705%	
Location 3	35%	114%	
Assumed same percentual change in CSR fatigue life in years			
	AH47	AH70	AH70 HFMI
Location 3	22.6 a	7.9 a	25.7 a

The comparison of fatigue lives shows the reduced fatigue life when using high strength steel AH70. The fatigue life reduces to around half of the original, in locations 2 and 3 even less than half of the original. When applying HFMI treatment, the fatigue life increased compared to the fatigue life of AH47 midship section.

As CSR fatigue life calculates fatigue life in years and considers the long-term distribution of loads (IACS 2019b, Pt 1, Ch 9, Sec 1, p. 4) 4R calculation cannot be compared directly with CSR fatigue life. Same percentual difference is assumed for the change in CSR fatigue life that was assumed in 4R fatigue lives of location 3, even though the CSR fatigue calculation does not include the effect of residual stress.

4.7 Unit weights

Weight calculations are done based on the unit weight obtained from RulesCalc as described in Section 3.9. The unit weight for midship sections made using AH47 and AH70. The assumed weight loss calculation is made as described in Section 3.9.

The unit weights are presented in Table 14. In the same table the assumed weight loss number is presented. If the percentual value of the weight loss $W\%$ is positive, there are achieved weight savings, if the value is negative there are weight gains.

Table 14. Weight comparison

Weight savings per unit length			
W.700	68521	kg/m	Unit weight, AH70 steel is used
W.470=	79927	kg/m	Unit weight, AH47 steel is used
W%=	14.3	%	

Presented values are weight of one meter of parallel midship structure. Over 14% weight saving could be achieved by using AH70 steel compared to midship section where AH47 steel is used. The relevancy of obtained weight saving is discussed in Section 5.2.

5 ANALYSIS AND DISCUSSION

Results presented in Chapter 4 are analyzed and discussed in this Chapter. The key findings of the study are analyzed and further discussed. Not all individual results are analyzed as they are part of the key results and findings. Further study that is planned to investigate AH70 fatigue properties is briefly described in Subsection 5.2.1.

5.1 Analysis of key results

Based on the results, AH70 steel can be used in the designed midship section, but much less than was expected. Originally it was expected that AH70 steel could be used in side shell plating, double side plating and in longitudinal stiffeners in bottom and main deck structures. AH70 steel could not be utilized in these locations to reduce plate thicknesses and stiffener scantlings. With the used assumptions and exclusions, AH70 steel could only be used in the ice strengthening structure to gain benefit. The used assumptions are conservative as other parts than the midship section of the ship are not designed.

Reason to the small use of AH70 steel was the limit for moment of inertia. The initial midship section with AH47 steel has a moment of inertia value of about 108.8% of the limit and at the same time the highest stress at hatch coaming is around 2% less than the limit value. When dimensioning the midship section with AH70 steel, the same 2.36% value below stress limit was set as design goal. The design goal could not be reached as the moment of inertia reached its limit value before stress value. The moment of inertia value of the midship section designed using AH70 steel is 0.11% over the limit. This is the main reason why AH70 steel could not be utilized more in the midship section, and the reason for the rejection of the hypothesis made in subchapter 1.6 of obtaining large weight savings in main deck area.

The material capacity of AH70 is used only around 87%. This suggests that the stresses in the structure could be increased even more when using AH70 steel. Increase of stress could not be achieved by lowering the moment of inertia when using lower plate thicknesses, but the bending moments of the ship could be increased.

As a result of weight savings, 14% of the original weight could be saved by using AH70 steel. The saving is made only by reducing scantlings of ice strengthened structure. After reducing the ice strengthened structure by using AH70 steel, the moment of inertia value was at the limit and no more reductions on the scantlings could be made.

The fatigue life of the midship section with AH47 steel was first calculated using the rule-based method. The calculated fatigue life exceeds the required fatigue life of 20 years. The fatigue life calculation procedure described in the CSR suits well as a reference calculation for the 4R method, as the CSR procedure is commonly known. It is still noted that the CSR based fatigue life calculation is designed for oil tankers and bulk carriers and is usually not used for container ship design.

When calculating fatigue life for midship with AH47 steel and with AH70 steel using 4R method, a fatigue life reduction was found. Fatigue life reduced almost to the half of the original fatigue life when using AH70 steel. There were two main reasons behind the reduction of fatigue life.

First reason for the reduction of fatigue life was the reductions in midship section cross section moment of inertia and section modulus when using AH70. The scantlings could be reduced with the use of higher strength steel. This led to reduction of cross-sectional area, then moment of inertia and section modulus which led to increase of stresses in the cross section.

Second reason for the fatigue life reduction is residual stress due to welding. 4R method considers the residual stresses in the joint after welding. The residual stresses are assumed to be equal to the yield strength of material based on the findings of Gannon et al. (2012, p. 33) and Kenno et al. (2010, pp. 272-273). When moving from AH47 to AH70 the tensile residual stresses are expected to rise from 460 MPa to 690 MPa. This results in increasing of stress range and to reduction in fatigue life.

On the other hand, the fatigue life increased drastically when applying HFMI treatment to the weld and the increase was larger than expected. All locations have higher fatigue life

than in the midship section made using AH47 steel. The AH47 midship section was assumed not to have HFMI treated welds.

The results are in line with the vertical location of a critical joint in the midship section. The location 3 has the largest external stress range and location 1 has the lowest. For this reason, it is reasonable that the location 3 has the smallest increase in fatigue life as it is subjected to large external stresses.

5.2 Discussion of results

As found out weight savings could be made by using AH70 steel, but the weight savings were achieved solely by using high strength steel as a material of ice strengthened structure. This suggests that there may not be practical use of high strength steels in an open water container ship when trying to lighten hull structure. If the cargo mass of the vessel could be increased, then the AH70 steel could be utilized to increase the permissible stresses. Heavier cargo could lead to higher bending moments which could lead to higher stresses while the midship section still satisfies the moment of inertia requirement.

14% weight saving is a large saving when thinking of the steel needed to construct a ship. The weight saving could bring fuel savings to the ship owner either by using less fuel to carry the same cargo than before or by using the same amount of fuel than before and carrying more cargo. The benefit of saving fuel is not only economical, but also environmental. As reviewed by the United Nations (2019, p. 4), a major part of all trade happens by sea. If an environmental impact of construction and operation of even a part of all the ships could be reduced, the total reduction in environmental impact could be significant.

Many of the container vessels operate on routes that are clear of ice i.e. Suez Canal. As found out in this study, weight savings could be achieved by lowering scantlings of ice strengthened structure. Because of that the same weight saving strategy cannot be applied to open-water vessels. As climate warming melts ice on the polar regions, Northern Sea route could become available for year-around use. Shipping companies have already started to investigate the use of Northern Sea Route as in 2018 a container ship *Venta Maersk* sailed through the Northern Sea Route as a trial (A.P. Moller-Maersk 2018). As the container trade

through the Northern Sea Route may increase, the use of AH70 steel to lower ice strengthening scantlings could be a powerful way of reducing environmental impact of shipping on the new trade route.

Increased strength of the longitudinal structure when using AH70 could allow more container tiers to be carried without increasing the ships main dimensions. Currently containerships have increased in length and breadth to carry more containers as noted by Prokopowicz and Berg-Andreassen (2016, p. 2915). Current shipping containers can be piled up to ten tiers. If the amount of cargo onboard is increased without increasing the ships length or breadth, a container would be needed that could withstand the weight from more tiers than ten. This restricts the increasing the height of the ship when carrying currently used containers.

Container ships are inertia limited ships due to their structural layout. The traditional layout of container ships has large deck openings to allow efficient container loading and unloading. The change from this layout would not be feasible as majority of the container handling equipment and the containers themselves are designed to operate with common types of container ships. This suggests that high strength steels could have a major use in other ship types like multi-deck ships where moment of inertia is not usually driving the design.

The length of the ship affects the inertia requirement directly as in equation 8 and by design bending moment according to equation 10. As the length of the ship increases, the required moment of inertia increases. As the moment of inertia requirement was driving the design in this study, it suggests that the ship was too long in order to gain full benefit from AH70 steel. On the other hand, the rule wave bending moment increases as the ship's length increases. By increasing the length of the ship, higher hull girder stresses are present in the structure. Higher stresses can be permitted by using steel with higher yield strength. There may be an optimal length for the ship where the moment of inertia is not driving the design, but the bending moments are high enough to justify the use of AH70 steel.

In the study the midship section of a container ship was assumed to be parallel trough out the studied length of the ship. As container ships operate in open waters, speed is an

important factor in the design and operation of a container ship. For this reason, the container ships tend to have a very short parallel midship section compared to their overall length. For an ice-breaking container ship on the other hand, the hull form could have a prismatic midship section assumed in this study.

Ice-breaking or arctic container ship may also have a completely different layout and container arrangement. Current containerships tend to have a fully cellular container arrangement. It may be possible that containerships that operate in the arctic would have way different container stowage system due to harsh environment conditions than current open water containerships have. High strength steel with 690 MPa yield strength could bring benefits to these new arrangements by allowing the design to be made from less steel with higher strength.

The assumption that the ship is constantly in one loading condition causes the still water bending moment to be quite large trough out the ship's lifetime. Still water bending moment causes mean stress for cyclic loading. The mean stress effects the ship's fatigue life significantly. It also causes the applied stress ratio R to be positive. The used assumption is conservative and in real life situation the still water bending moment of a ship changes as the loading changes. The use of actual loads from simulated or measured data in the design process and fatigue calculations, could reveal more benefits of using high strength steel.

Residual stress had also a great effect on fatigue life as it was assumed that no post weld treatments would be used, and worst-case scenario of residual stress was used. Effect of residual stress on lowering the fatigue life is greater when using AH70 steel than when using AH47 steel as the residual stress is linked to the yield strength of material. In real welding the residual stresses may be smaller than the worst-case assumption or there may be relocating of the residual stresses. Effect of this on ice strengthened structure would be desirable to study.

On the other hand, the residual stress assumed after HFMI treatment is also linked to material. As residual stress after HFMI treatment is assumed to be a fraction of the ultimate strength of the material and compressive, higher material ultimate strength leads to higher compressive residual stress. In location 1 the mean stress is on compressive side which leads

to very high fatigue life. Same type of finding of increasing fatigue life by modifying residual stress is made by Cheng et al. (2003).

Farajian, Nitschke-Pagel and Dilger (2010) found out that the residual stresses after welding are not as high compared to the material yield strength than with milder steels. They observed that the residual stress after welding a S690 steel was around 500 MPa at the maximum (Farajian et al. 2010, p. 369). This would suggest that the used assumption of residual stress is conservative compared to the actual residual stresses. Farajian et al. (2010) conducted the test on small pieces and observed residual stress relaxation. In a ship's structure there are a lot of structural members connecting to each other compared to a test specimen. It may be that in a ship structure, the residual stresses are higher than Farajian et. al. (2010) observed as the surrounding structures may restrict the deformation after welding causing residual stresses.

As found out the HFMI treatment of welds can increase fatigue strength of a welded joint drastically. Fatigue strength could be improved in ship structures by using high strength steels and introducing post-weld treatments into manufacturing process. As ship has a lot of welds, the cost benefit would need to be evaluated if it is more beneficial to use light structure with high strength steels and use post-weld treatments to modify residual stresses, or to use current steel grades and leave the welds to as-welded condition. It could be reasonable to use AH70 steel and apply post weld treatments only to the joints that would need improved fatigue strength. By this way, the benefit of AH70 steel would be obtained and the work needed to conduct the post-weld treatment would be minimized. Also, a different post weld treatment method could be applied. As the applied residual stress ratio is relatively high, it may be that HFMI treatment is not the best post weld treatment.

4R method is a novel method and can consider the material strength in fatigue assessment. The method could be used in the future for design light structures using high strength steels in ship construction. The effect on fatigue strength of introducing new high strength steels could then be evaluated in early stage of design process.

5.2.1 Further study to be conducted

In order to implement high strength steel AH70 into an actual design of ships more research on the subject is needed. As there are no designs made yet using AH70 steel as a hull construction material, additional study on the high strength steel use would be beneficial. Even some of the aspects would be a part of a normal design process of a container ship, additional studies could be beneficial to do before starting a project of designing a container ship using AH70 steel.

Assumed challenges for the use of AH70 and the items excluded from the study are important to study before the full benefit of the AH70 steel could be gained. Items listed in the Table 1 in subchapter 1.2 and in the Table 2 in subchapter 1.5.1 could act as good starting points for further studies. Few of the most important items are described further. These items are locations and structural members of the ship that are not considered in this study, buckling and limits given by the rule sets.

Locations of the ship that are excluded from the study, could benefit from the use of AH70 steel. I.e. AH70 steel could be utilized in the bow region as the bow is subjected to multiple loadings like loads from bow flare. Local scantling limits could also be satisfied by using higher strength steels in plates with lower thickness. I.e. ballast tank boundaries may benefit from AH70 steel. In a container ship, the hatch covers may also be places where the use of AH70 steel would be beneficial.

Buckling aspects of using high strength steels would need more studying before using high strength steel in a ship. This study is not focusing on buckling, but when using smaller scantlings in structures buckling may become an issue and therefore it is desirable to address in future studies. Buckling can be a problem in a ship structure as structural members are subjected to high compressive loading as well as lateral loading i.e. ice pressure on ships side shell.

Main issue when using high strength steel in a container ship is a moment of inertia requirement. Required moment of inertia is a fundamental property of ship structural design process. In order to use high strength steel to produce weight savings in an open water container ship, moment of inertia of the ship may have to be lowered below the rule

requirement. Further study would be desirable if the moment of inertia limit could be lowered safely for a container ship with a certain structural layout.

Important item to study is the design loads. By using actual loads and actual residual stresses in the study the benefits of high strength steel could be studied more precisely. Measured loads from an existing ship could be used in the study. Also, numerical simulations like spectral analysis could be used to determine loads that are closer to the actual loads. On the other hand, the ship needs to comply with the rules in order to get a classification and to ensure the safety of the ship. The use of actual loads in the study could also affect the need of post weld treatments in cyclic loaded joints.

Ship manufacturing from a high strength steel like AH70 is also desirable to study. Manufacturing is a crucial part in a ship building process and it can have a large effect on the quality and fatigue properties of joints. Manufacturing also affects the cost of a ship made from high strength steel.

The cost of a ship needs to be reasonable when using high strength steel. A study of the cost impact of building a ship using high strength steel could be beneficial. The use of high strength steel could increase the manufacturing costs at the beginning, but after establishing manufacturing practices for the new material, the cost of production could be lowered. High strength steel could also lower the operating costs of the ship by making the ship lighter. The reduced mass of the ship's structures could also lower the recycling cost of the ship and help to meet the tightening environmental requirements in the future. A study of the environmental impact of using high strength steel would also be desirable.

Aker Arctic Technologies is planning to conduct a fatigue test together with LUT University to study more about the effect of material strength on fatigue capacity. Two test specimens are planned to be manufactured with a geometry based on the joint geometry of location 1 of this study. Specimens are planned to be manufactured from AH47 and AH70 steels and loaded with similar loadings to see the effect of new material on fatigue in joint typical to ship structures.

6 CONCLUSIONS

The main goal of the study was to find out if AH70 high strength steel with yield strength of 690 MPa could be used to design a container ship. It was studied if the AH70 steel could be used in longitudinal structures loaded by global bending moments. The motivation for the study is that Aker Arctic Technologies is a part of a research project to study the use of high strength steels in ship construction. High strength steel use would lower the weight of a ship freeing more space for cargo and lowering the emissions and costs of freight as well as emissions rising from manufacturing of the ship.

The study was focused on finding if it is possible to design an ice strengthened container ship from AH70 steel and is there fatigue problems arising when using AH70 steel instead of AH47 steel. Finally, it was studied if weight savings could be obtained with the use of AH70 steel. In order to solve these objectives, the study had three research questions. The research questions in the study were:

1. How to design longitudinal strength of an ice strengthened container ship when using high strength steel as a construction material?
2. Will the use of high strength steel lead to fatigue issues?
3. Is there weight savings to be achieved by using high strength steels in design?

It was found out that the longitudinal strength of an ice strengthened container ship can be designed by using AH70 steel by following the limits described by the UR-S11A. The same design principle can be made, but new material factor k_L value needs to be included into the design process. Scantlings of ice strengthening structure can be lowered with the use of AH70 steel, but other scantlings cannot be lowered compared to a design made using AH47 steel. In the design the driving factor is the moment of inertia of midship section. The moment of inertia limit is a fundamental part of current rule sets which ensure the safety of the ship. Due to the moment of inertia other scantlings than ice strengthened could not be lowered by allowing higher stresses in the member. Higher stresses could be allowed by using AH70 steel with yield strength of 690 MPa.

The use of AH70 steel was found to lead to reduction of fatigue life of the midship section. The calculated fatigue life reduced almost to a half of the fatigue life of design made using AH47 steel. The fatigue life was calculated using a novel fatigue life calculation method called 4R method. The method considers the residual stresses in connections as well as the strength of the used material.

Fatigue life of the midship section designed using AH70 steel could be increased by introducing post weld treatments. HFMI treatment was considered as a method of post weld treatment and it was considered numerically in the 4R fatigue life calculation. With the use of HFMI treatment, the fatigue life of section made from AH70 steel could be increased to be more than the fatigue life of the same midship section designed using AH47 steel.

Around 14% weight saving could be achieved per meter of parallel midship section when using AH70 steel in ice strengthened structures instead of AH47 steel. The obtained weight reduction is significant when related to the entire lightship weight of the ship. The scantlings of other structures could not be lowered to bring notable weight savings.

LIST OF REFERENCES

Ahola, A. & Björk, T. (2020). On the stress concentrations of fillet-welded joints - Numerical study on the longitudinal gussets (under work).

Ahola, A., Skriko, T. & Björk, T. 2019. Fatigue analysis on the transverse fillet-welded joints made of ultra-high-strength steel – mean stress correction using 4R method. International Institute of Welding (IIW) document XIII-2779-19. Lappeenranta-Lahti University of Technology LUT. Lappeenranta. 17 p.

A.P. Moller-Maersk. 2018. [Press release] Maersk concludes trial passage of Northern Sea Route. 2 p.

Bai Y. & Wei-Liang J. 2016. [Part 1:] Marine Structural Design Second Edition. Houston: Elsevier Inc. 955 p.

Björk, T., Mettänen, H., Ahola, A. et al. 2018. Fatigue strength assessment of duplex and super-duplex stainless steels by 4R method. *Welding in the World* (2018) 62: 1285. Springer Berlin Heidelberg. doi: <https://doi.org/10.1007/s40194-018-0657-8>

Cheng, X., Fisher, J. W., Prask, H. J., Gnäupel-Herold, T., Yen, B. T. & Roy, S. 2003. Residual stress modification by post-weld treatment and its beneficial effect on fatigue strength of welded structures. *International Journal of Fatigue*, 25(9-11), pp. 1259-1269. doi:10.1016/j.ijfatigue.2003.08.020

Committee on Large Container Ship Safety. 2013. Interim Report of Committee on Large Container Ship Safety (English version). Safety Policy Division, Maritime Bureau, Ministry of Land, Infrastructure, Transport and Tourism. Japan. 66 p.

DNVGL-CG-0129. 2018. Class Guideline, Fatigue Assessment of ship structures. DNV GL AS. 235 p.

Dowling, N. E., Siva Prasad, K. & Narayanasamy, R. 2013. Mechanical behavior of materials: Engineering methods for deformation, fracture, and fatigue. 4th ed., international ed. Harlow: Pearson Education. 945 p.

Edward, V. 1988. Principles of Naval Architecture Second Revision: Volume 1, Stability and Strength. Jersey City: The Society of Naval Architects and Marine Engineers (SNAME). 310 p.

Farajian, M., Nitschke-Pagel, T. & Dilger, K. 2010. Mechanisms of Residual Stress Relaxation and Redistribution in Welded High-Strength Steel Specimens under Mechanical Loading. *Welding in the World*, 54(11), pp. R366-R374. doi:10.1007/BF03266751

Gannon, L., Liu, Y., Pegg, N. & Smith, M. J. 2012. Effect of welding-induced residual stress and distortion on ship hull girder ultimate strength. *Marine Structures*, 28(1), pp. 25-49. doi:10.1016/j.marstruc.2012.03.004

Hobbacher A. 2014. International Institute of Welding (IIW) Recommendations for fatigue design of welded joints and components. IIW Document IIX-xxx-13 ex XIII-2460-13/XV-1440-13. Paris. 146 p.

Hong, S. J. 2019. Lead Specialist, Structure Group, Busan Technical Support Office, Lloyd's Register. Skype Meeting 30.10.2019

Hughes O. & Paik J. 2010. Ship Structural Analysis and Design. Society of Naval Architects and Marine Engineers (SNAME). Jersey City. 606 p.

IMO Maritime Environment Protection Committee. 2010. [Chapter 4:] Regulations on Energy Efficiency for Ships. In: Revised MARPOL ANNEX VI Regulations for the Prevention of Air Pollution from Ships.

IMO Maritime Safety Committee. 2014. 'Resolution MSC.385(94) of 21 November 2014' International Code for Ships Operating in Polar Waters (Polar Code). 52 p. Available at:

<http://www.imo.org/en/MediaCentre/HotTopics/polar/Documents/POLAR%20CODE%20TEXT%20AS%20ADOPTED.pdf>

International Association of Classification Societies (IACS). 2019a. Common Structural Rules 01 June 2019.

International Association of Classification Societies (IACS). 2019b. Common Structural Rules Technical Background Rule Reference.

International Association of Classification Societies (IACS). 2017. Nr. 84 Container ships – Guidelines for Surveys, Assessment and Repair of Hull Structures – Rec. 2005/Rev. 1 2017. 145 p.

ISO 668. 2013. Series 1 freight containers. Classification, dimensions and ratings. 6th edition. Geneva: International Organization for Standardization. 7 p.

Lamb, T. 2003. Ship design and construction Volumes 1 – 2. The Society of Naval Architects and Naval Engineers (SNAME). 883 p.

Li, Z., Mao, W., Ringsberg, J. W., Johnson, E. & Storhaug, G. 2014. A comparative study of fatigue assessments of container ship structures using various direct calculation approaches. *Ocean Engineering*, 82(1), pp. 65-74. doi:10.1016/j.oceaneng.2014.02.022

Lloyd's Register (LR). 2019. Rules and Regulations for the Classification of Ships. Lloyd's Register Group Limited. London. 1753 p.

Lloyd's Register (LR). 2018. ShipRight Design and Construction, Structural design assessment, Global Design Loads of Container Ships and Other Ships Prone to Whipping and Springing. Lloyd's Register Group Limited. London. 57 p.

Lloyd's Register (LR). 2017. Fatigue Design Assessment – Application and Notations. Lloyd's Register Group Limited. London. 30 p.

Lloyd's Register (LR). 2009. ShipRight Design and Construction, Fatigue Design Assessment – Level 1 Procedure Structural Detail Design Guide. Lloyd's Register. 135 p.

Mansour, A. & Liu, D. 2008. [Chapter 2:] Principles of Naval Architecture Series - Strength of Ships and Ocean Structures. Society of Naval Architects and Marine Engineers (SNAME). Jersey City. 208 p.

Marquis, G. B. & Barsoum, Z. 2016. IIW Recommendations for the HFMI Treatment: For Improving the Fatigue Strength of Welded Joints. Singapore: Springer Singapore.

Molland, A. 2008. The Maritime Engineering Reference Book, A Guide to Ship Design, Construction and Operation. Elsevier Ltd. Burlington. 902 p.

Parmentier, G. & Huther, M. 2013. S-N Curves for Welded, Non-welded or Improved Welded Details of Marine Structures. Procedia Engineering, 66(C), pp. 49-61. doi:10.1016/j.proeng.2013.12.061

Prokopowicz, A. K. & Berg-Andreassen, J. 2016. An Evaluation of Current Trends in Container Shipping Industry, Very Large Container Ships (VLCSs), and Port Capacities to Accommodate TTIP Increased Trade. Transportation Research Procedia, 14, pp. 2910-2919. doi:10.1016/j.trpro.2016.05.409

Sumi, Y., Yajima, H., Toyosada, M., Yoshikawa, T., Aihara, S., Gotoh, K., Morikage, Y. 2013. Fracture control of extremely thick welded steel plates applied to the deck structure of large container ships. Journal of Marine Science and Technology, 18(4), pp. 497-514. doi:10.1007/s00773-013-0222-5

United Nations. 2019. Review of Maritime Transport 2019. UNCTAD United Nations on Trade and Development. Geneva. 108 p.

UR-S4. 2010. Criteria for the Use of High Tensile Steel with Minimum Yield Stress of 315 N/mm², 355 N/mm² and 390 N/mm² - Rev.3 May 2010 Clean. International Association of Classification Societies (IACS). 1.p

UR-S11A. 2015. Longitudinal Strength Standard for Container Ships June 2015. International Association of Classification Societies (IACS). 21.p

Vladimir, N., Malenica, S., De Lauzon, J., Senjanovic, I., Im, H., Choi, B. & Cho, D. 2016. Structural Design of Ultra Large Ships Based on Direct Calculation Approach. Pomorski Zbornik, 1, pp. 63-79.

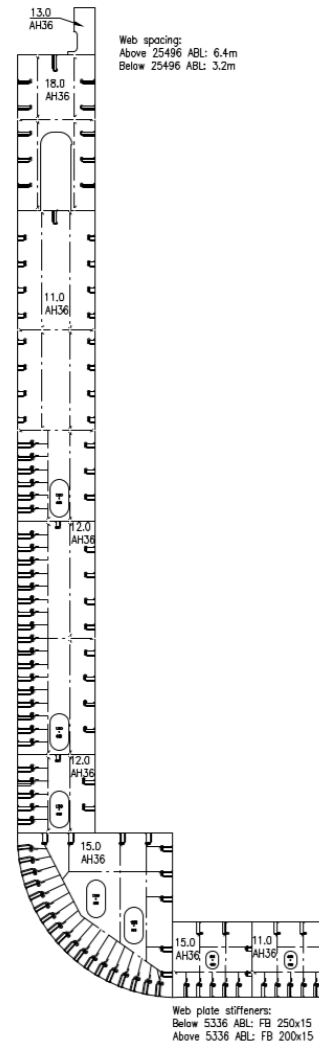
Zukauskaite, A., Mickeviciene, R., Kamauskaite, D. & Turkina, L. 2013. Environmental and humane health issue of welding in the shipyard. Transport Means - Proceedings of the International Conference, pp. 177-180.

UR-S11A section modulus and stress calculations, AH47

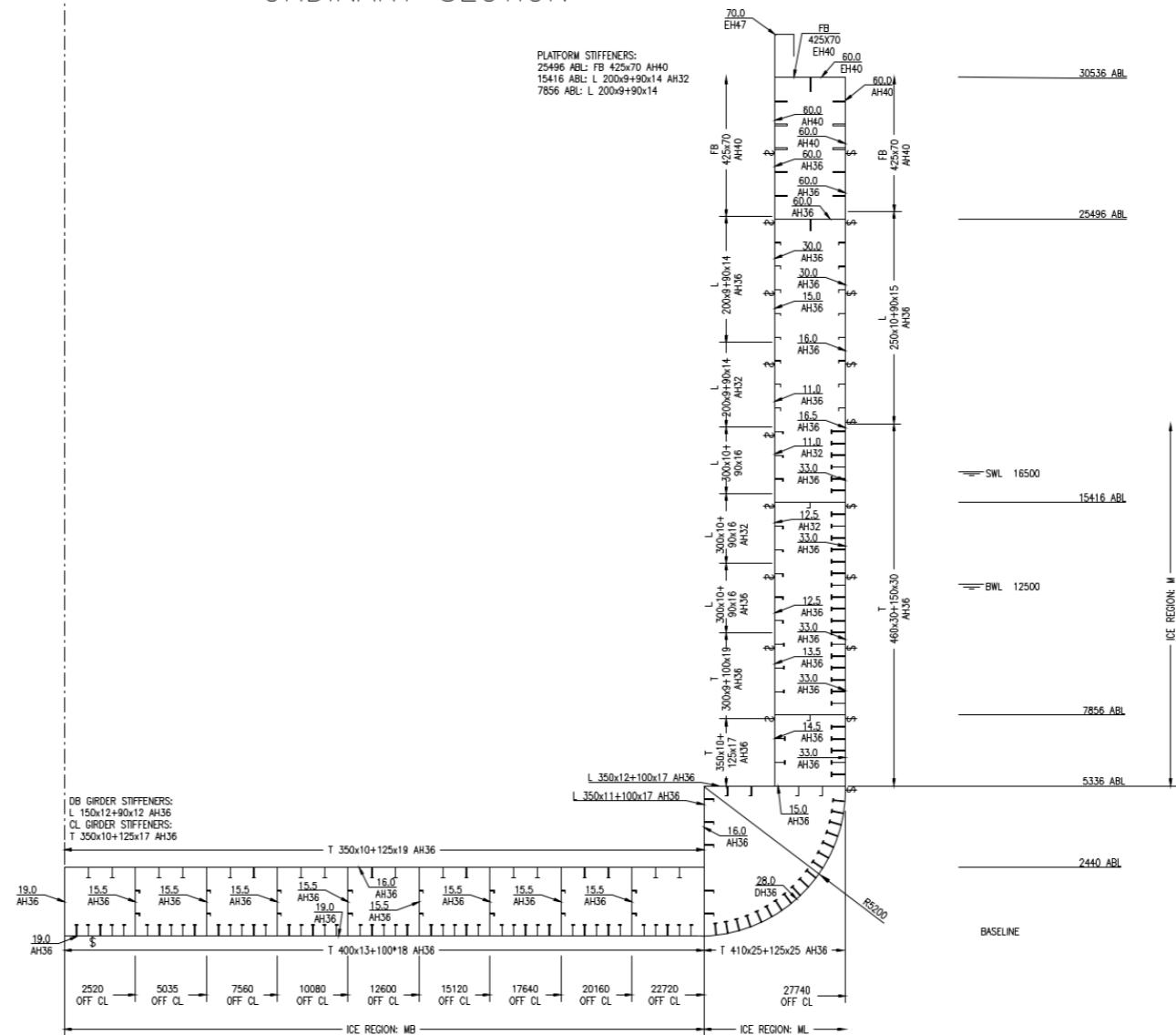
Bending stress calculation for UR-S11A for midship section from AH47			
Input value			
Permissible stress			
$\sigma_{perm} = \frac{R_{eH}}{\gamma_1 \gamma_2}$ $\gamma_1 = k \frac{R_{eH}}{235}$			
R.eh=	460	MPa	Yield strength of construction material
k=	0,62		k-factor for material
γ_1 =	1,21361702		Partial safety factor
γ_2 =	1,24		For bending strength assessment, according to 3.3.2
σ_{per} =	305,671176	MPa	Permissible stress
Minimum inertia requirement			
$I_{net} \geq 1.55L M_s + M_w 10^{-7}$			
M.s=	9200000	kNm	Still water bending moment, obtained from RulesCalc
M.w=	12402795,3	kNm	Rule wave bending moment, obtained from RulesCalc
L=	378	m	Rule length
I.net≥	1265,70777	m ⁴	Required moment of inertia
Bending stress			
$\sigma_{HG} = \frac{\gamma_s M_s + \gamma_w M_w}{I_{net}} (Z - Z_n) 10^{-3}$			
M.s=	9200000	kNm	
M.w=	12402795,3	kNm	
γ_s =	1		Partial safety factor
γ_w =	1		Partial safety factor
Z.n=	13,002	m	Location of neutral axis, obtained from RulesCalc
Z=	32,036	m	Vertical co-ordinate of location under consideration
I.act=	1376,970	m ⁴	Actual moment of inertia, obtained from RulesCalc
σ_{HG} =	298,617693	N/mm ²	
Check			
Inertia above limit?		Yes	by 8,79 %
Bending stress below permissible?		Yes	by 2,36 %

Bending stress calculation for UR-S11A for midship section designed using AH70			
Input value			
Permissible stress			
$\sigma_{perm} = \frac{R_{eH}}{\gamma_1 \gamma_2}$			
$\gamma_1 = k \frac{R_{eH}}{235}$			
R.eh=	690	MPa	Yield strength of construction material
k=	0,53		k-factor for material
γ_1 =	1,556170213		Partial safety factor
γ_2 =	1,24		For bending strength assessment, according to 3.3.2
σ_{per} =	357,5776019	MPa	Permissible stress
Minimum inertia requirement			
$I_{net} \geq 1.55L M_s + M_w 10^{-7}$			
M.s=	9200000	kNm	Still water bending moment, obtained from RulesCalc
M.w=	12402795,27	kNm	Rule wave bending moment, obtained from RulesCalc
L=	378	m	Rule length
I.net \geq	1265,707775	m ⁴	Required moment of inertia
Bending stress			
$\sigma_{HG} = \frac{\gamma_s M_s + \gamma_w M_w}{I_{net}} (Z - Z_n) 10^{-3}$			
M.s=	9200000	kNm	
M.w=	12402795,27	kNm	
γ_s =	1		Partial safety factor
γ_w =	1		Partial safety factor
Z.n=	13,642	m	Location of neutral axis, obtained from RulesCalc
Z=	32,036	m	Vertical co-ordinate of location under consideration
I.act=	1267,159	m ⁴	Actual moment of inertia, obtained from RulesCalc
σ_{HG} =	313,5848115	N/mm ²	
Check			
Inertia above limit?	Yes	by	0,11 %
Bending stress below permissible?	Yes	by	14,03 %

WEB SECTION



ORDINARY SECTION



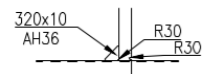
15000 TEU CONTAINER SHIP

Length, overall	abt. 400.0	m
Length, SWL (T 16.5 m)	378.0	m
Breadth, moulded	55.48	m
Displacement (DWL)	abt. 247 800	t
Ice class:	PC-3	

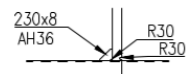
- NOTES:
1. Material grade "A" unless otherwise noted
 2. Stillwater bending moment Hogging 9 200 000 kNm
 3. All dimensions in mm

Longitudinal stiffener end connections:

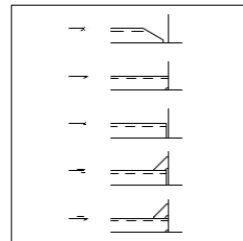
At bottom and bilge shell within ice region Mb and Ml:



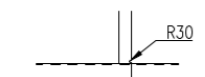
At side shell within ice region M:



Stiffener end symbols

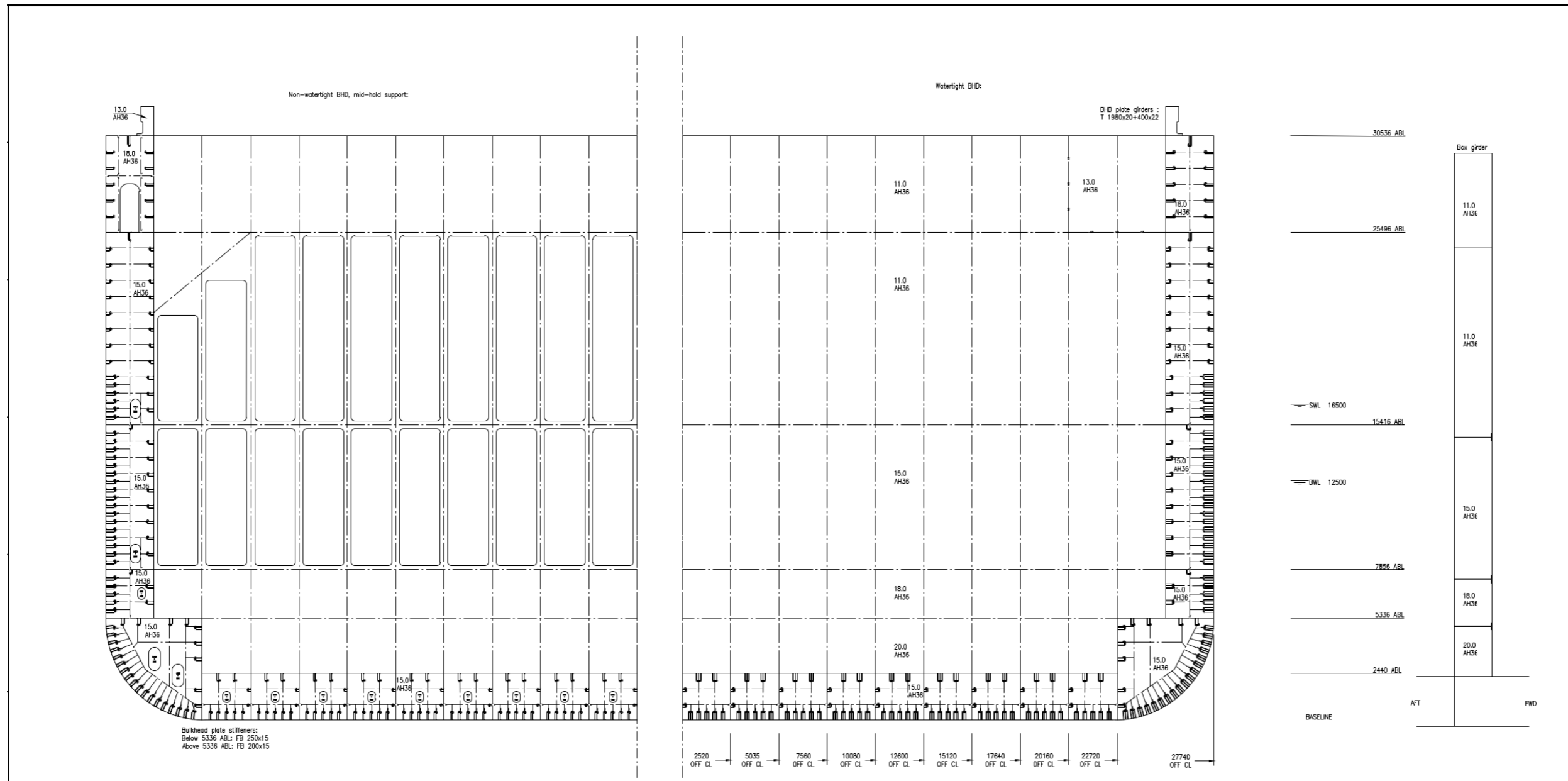


At inner bottom, inner bottom girders and bilge box:



Revision	2020-04-07	Alteration or Remark
Design Phase		
Confidentiality		Copyright of Aker Arctic Technology Inc. All rights reserved. No part, without prior written permission, shall be reproduced or transmitted in any form or by any means, electronic or mechanical, including photocopying, recording, or by any information storage and retrieval system, without the prior written permission of Aker Arctic Technology Inc.
Reference Drawing		Aker Arctic
Designer	Lindroos	Ship
Checked by		MIDSHIP SECTION
Reviewed by		
Approved by		
Aker Arctic Design	Sheet 1 of 1	Drawing Number
Paper Size A1 (594x841)	Drawing Scale 1:100	Revision Code

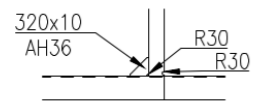
PRELIMINARY



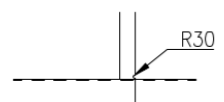
Bulkhead plate stiffeners:
Below 5336 ABL: FB 250x15
Above 5336 ABL: FB 200x15

Longitudinal stiffener end connections:

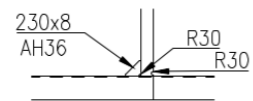
At bottom and bilge shell within ice region Mb and MI:



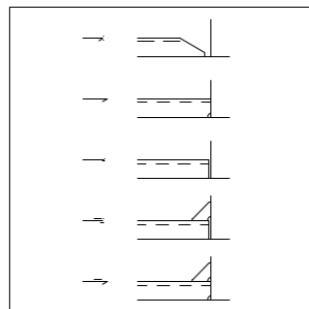
At inner bottom, inner bottom girders and bilge box:



At side shell within ice region M:



Stiffener end symbols



15000 TEU CONTAINER SHIP

Length, overall	abt. 400.0	m
Length, SWL (T 16.5 m)	378.0	m
Breadth, moulded	55.48	m
Displacement (DWL)	abt. 247 777	t
Ice class:	PC-3	

Bulkhead spacing: 12.8 m

Every second bulkhead is water tight bulkhead. Water tight bulkheads are located between cargo holds.

NOTES:

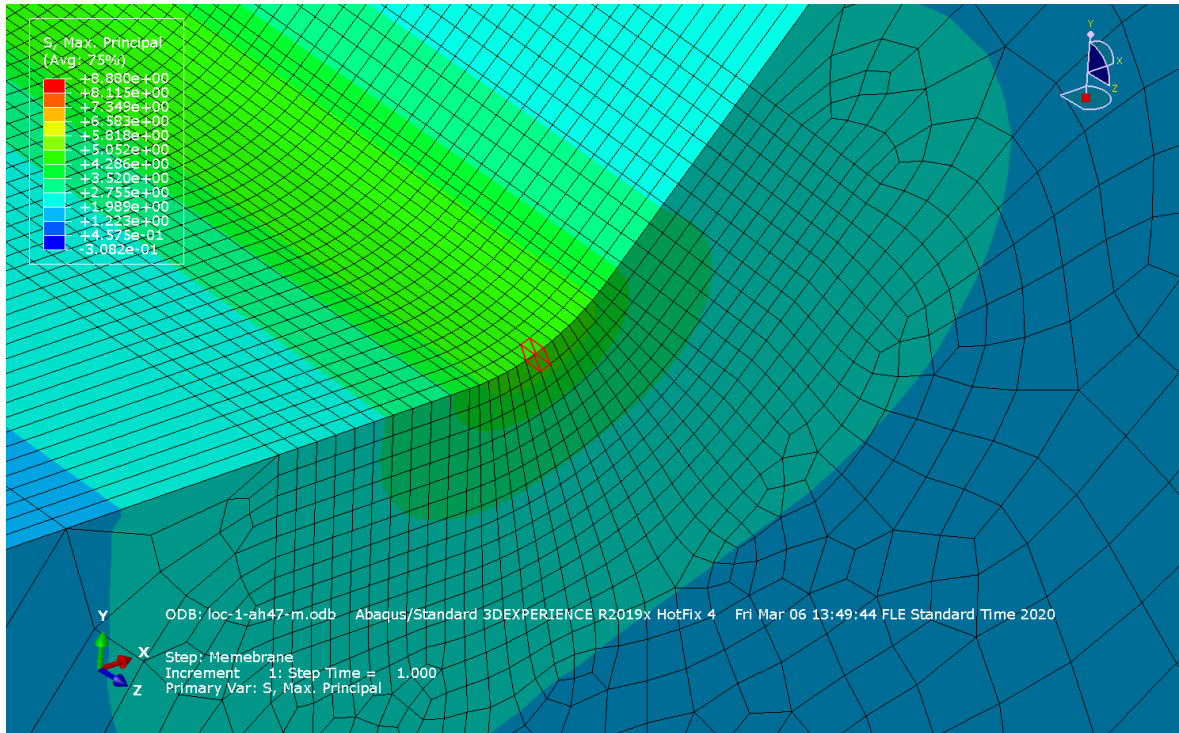
1. Material grade "A" unless otherwise noted
2. Stillwater bending moment
3. Hogging 9 200 000 kNm

All dimensions in mm

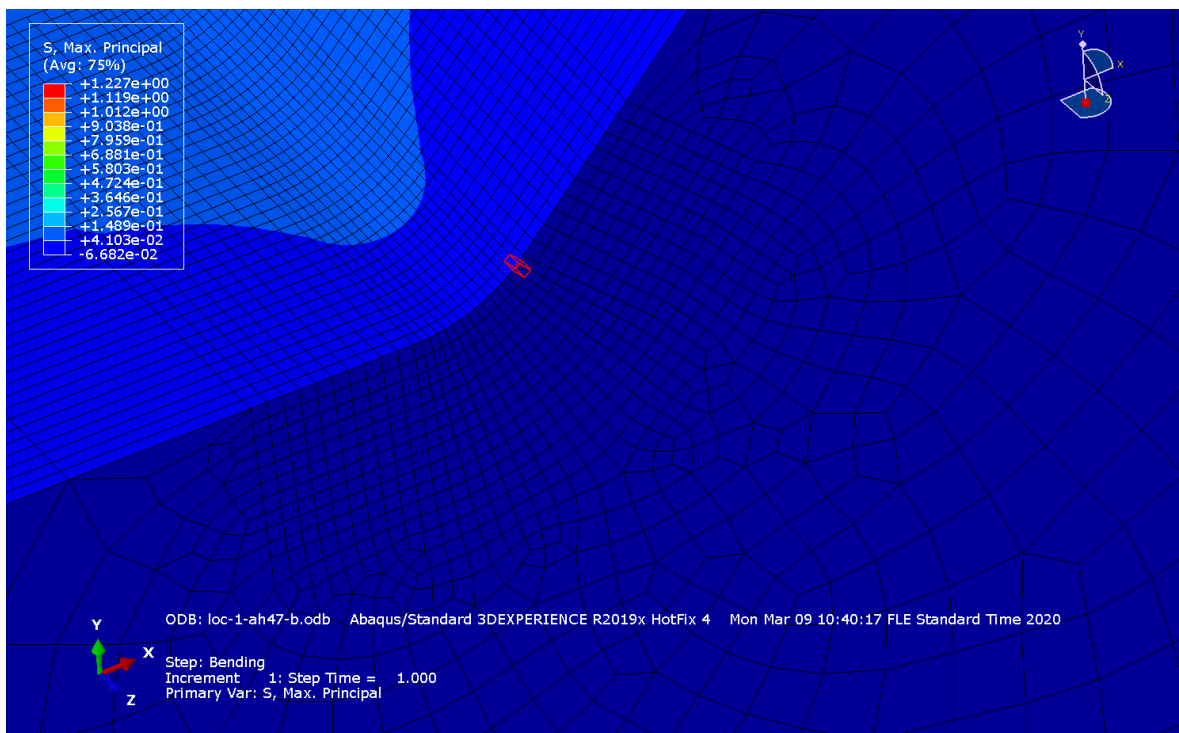
Revision	2023-04-07	Alteration or Remark
Design Phase		
Confidentiality	Copyright of Aker Arctic Technology Inc. All rights reserved. No part thereof may be electronic, duplicated or in any other way made use of, except with prior approval of Aker Arctic Technology Inc.	
Business Drawing		
Designer	Lindegaard	File
Checked by		BULKHEAD SECTION
Approved by		
Aker Arctic Design	Sheet	Drawling Number
Paper Size	Drwing Scale	Document Date
A1 (594x841)	1:100	

Aker Arctic
PRELIMINARY

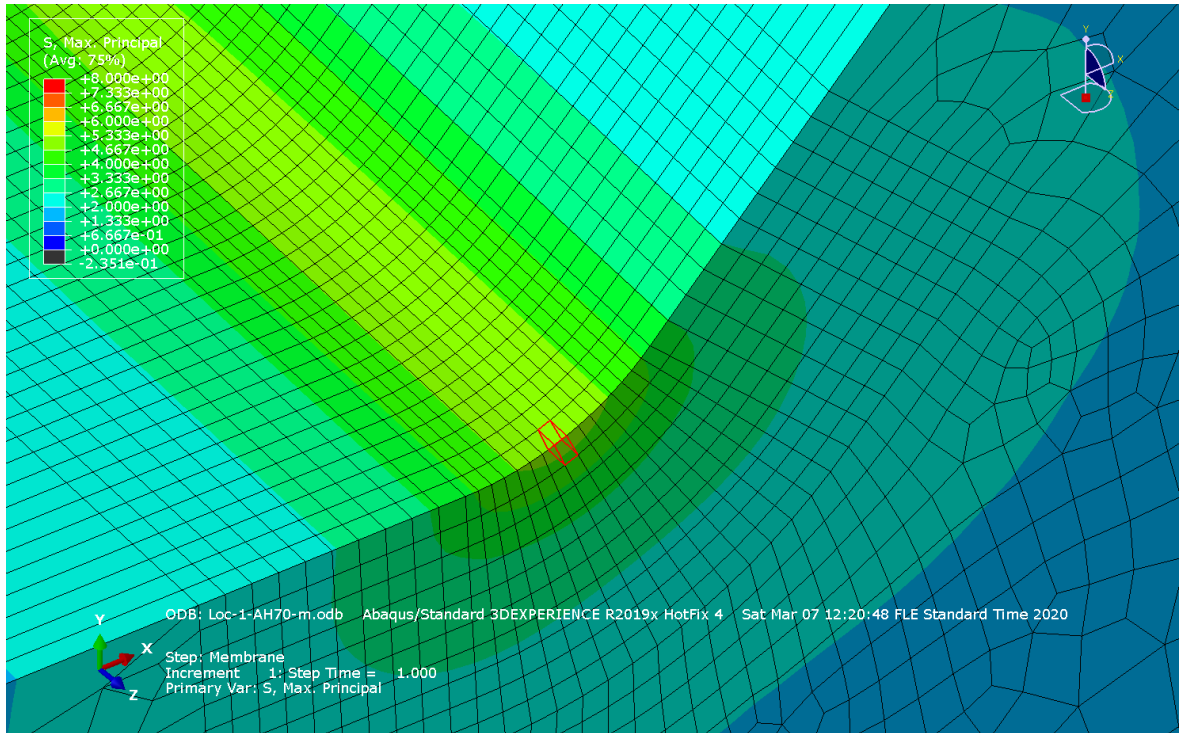
K_m of location 1 AH47



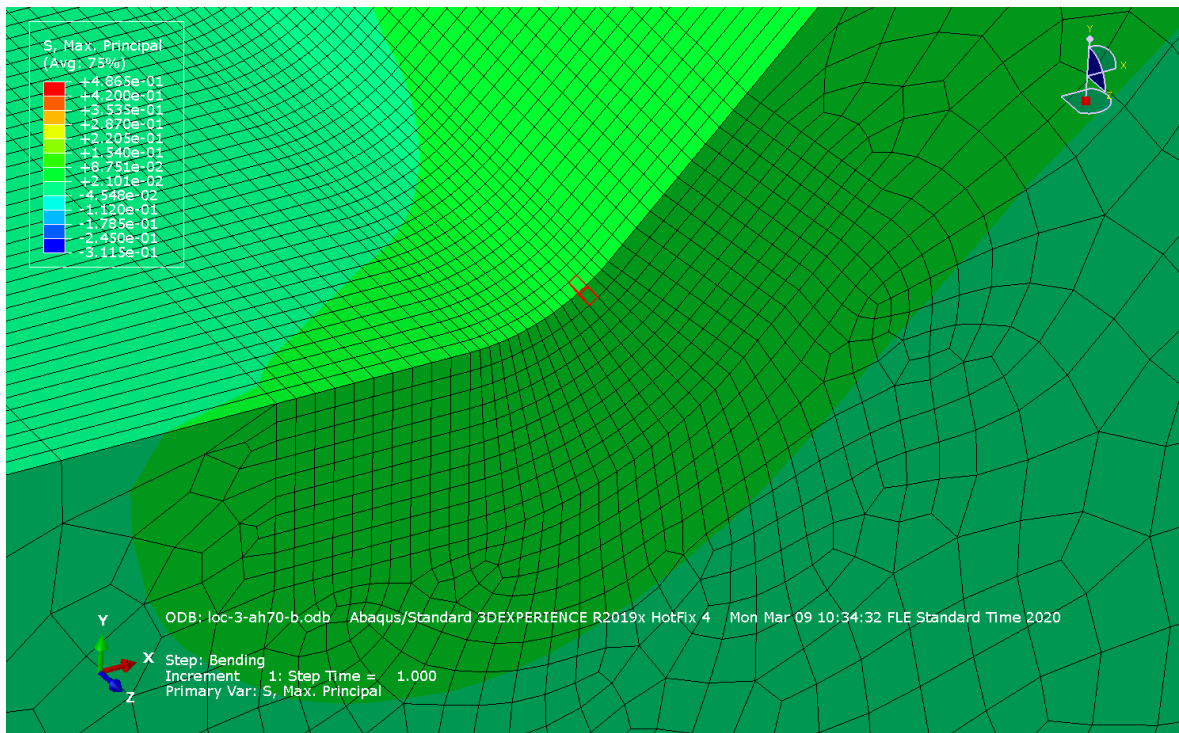
K_b of location 1 AH47



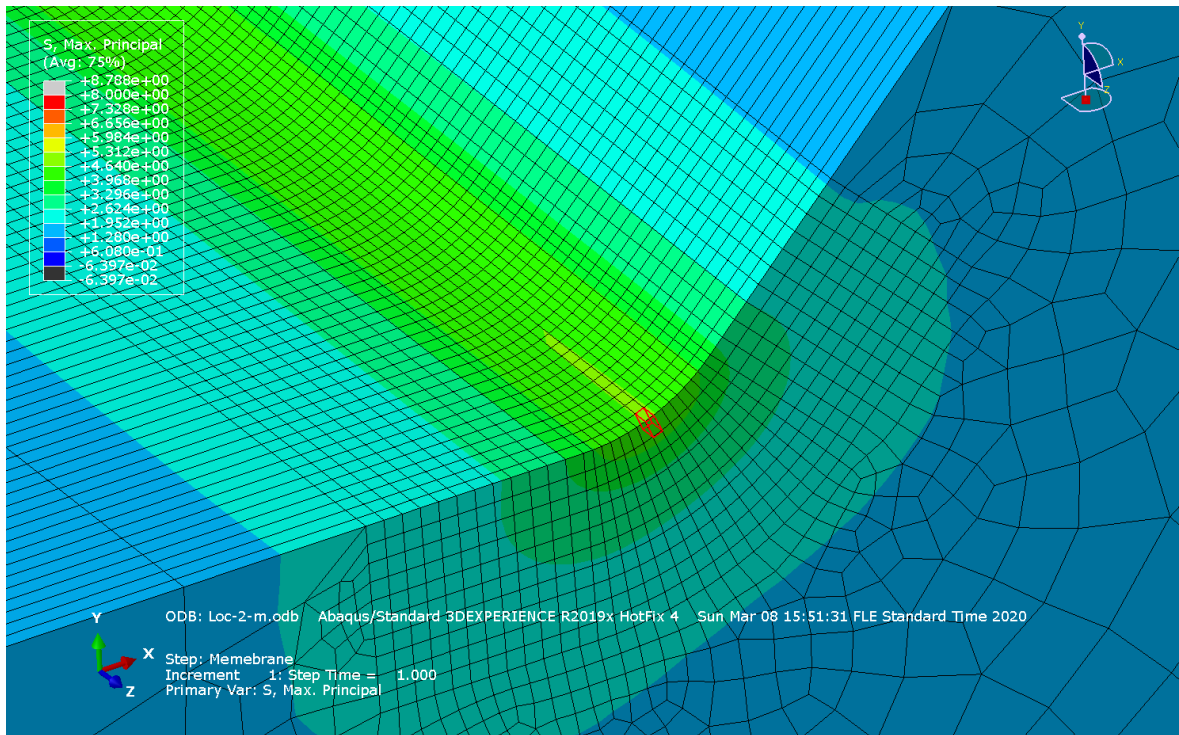
K_m of location 1 AH70



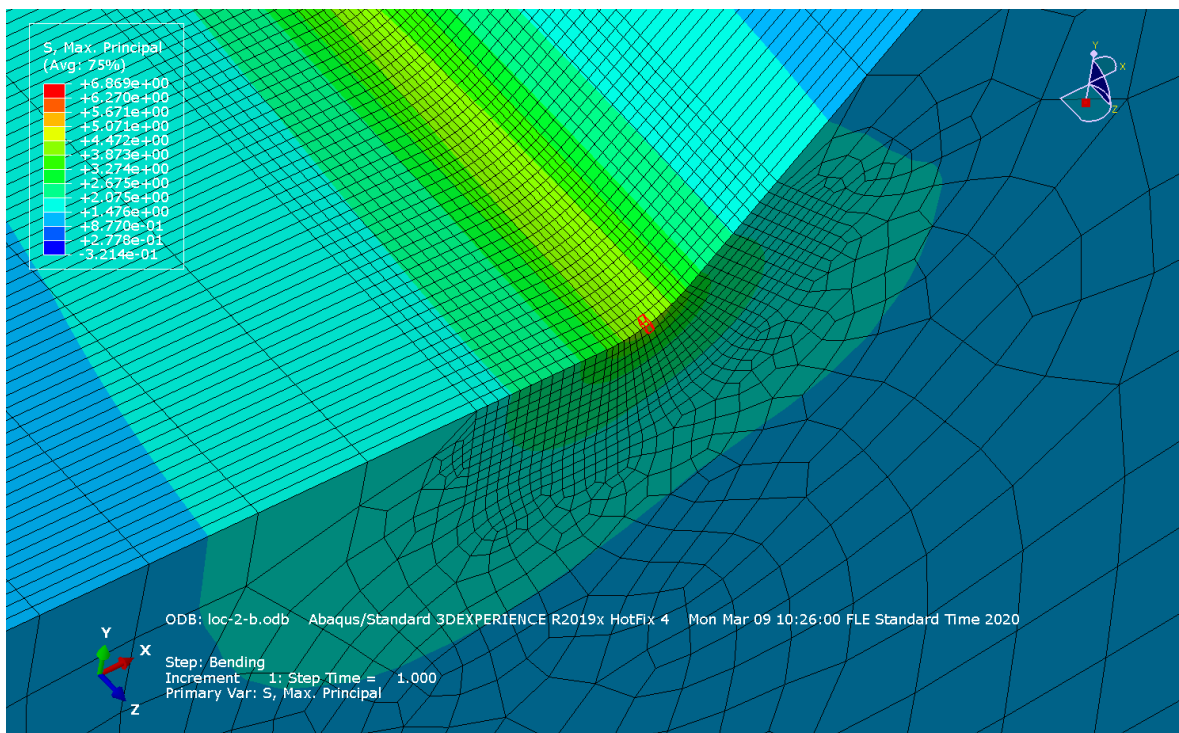
K_b of location 1 AH70



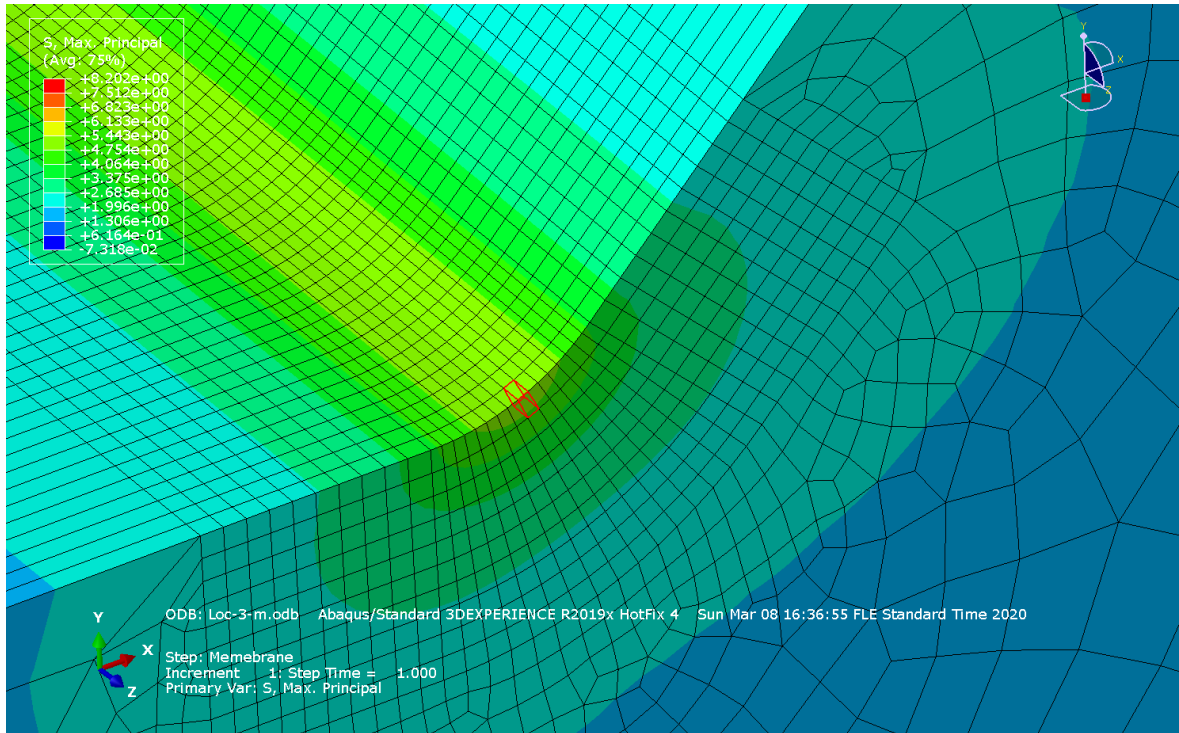
K_m of location 2



K_b of location 2



K_m of location 3



K_b of location 3

